Building Applied Photovoltaic Arrays:

Side-by-Side Array Comparison With and Without Fan Cooling

by:

Saurabh Chatterjee

A Thesis Presented in Partial Fulfillment
of the Requirements for the Degree
Master of Science in Technology

Approved November 2011 by the
Graduate Supervisory Committee:

Govindasamy Tamizhmani, Chair
Bradley Rogers
Narciso Macia

ARIZONA STATE UNIVERSITY

December 2011

ABSTRACT

Building Applied Photovoltaics (BAPV) form an essential part of today's solar economy. This thesis is an effort to compare and understand the effect of fan cooling on the temperature of rooftop photovoltaic (PV) modules by comparing two side-by-side arrays (test array and control array) under identical ambient conditions of irradiance, air temperature, wind speed and wind direction. The lower operating temperature of PV modules due to fan operation mitigates array non uniformity and improves on performance. A crystalline silicon (c-Si) PV module has a light to electrical conversion efficiency of 14-20%. So on a cool sunny day with incident solar irradiance of 1000 W/m^2, a PV module with 15% efficiency, will produce about only 150 watts. The rest of the energy is primarily lost in the form of heat. Heat extraction methods for BAPV systems may become increasingly higher in demand as the hot stagnant air underneath the array can be extracted to improve the array efficiency and the extracted low-temperature heat can also be used for residential space heating and water heating. Poly c-Si modules experience a negative temperature coefficient of power at about -0.5% /^{o}C. A typical poly c-Si module would experience power loss due to elevation in temperature, which may be in the range of 25 to 30% for desert conditions such as that of Mesa, Arizona. This thesis investigates the effect of fan cooling on the previously developed thermal models at Arizona State University and on the performance of PV modules/arrays. Ambient conditions are continuously monitored and collected to calculate module temperature using the thermal model and to compare with actually measured temperature of individual modules. Including baseline analysis, the thesis has also looked into the effect of fan on the test array in three stages of 14 continuous days each. Multiple

Thermal models are developed in order to identify the effect of fan cooling on performance and temperature uniformity. Although the fan did not prove to have much significant cooling effect on the system, but when combined with wind blocks it helped improve the thermal mismatch both under low and high wind speed conditions.

To my Dad, Mom & Parents in Law

To my Beloved Wife

ACKNOWLEDGMENTS

I would like to extend my sincere gratitude to Dr. Govindasamy Tamizhmani (Dr. Mani) for taking his time and interest and giving me an opportunity to work on this thesis. Without his continued support and guidance this project would not have been possible. I would like to thank my committee members, Dr. Bradley Rogers and Dr. Narciso Macia, for their valuable feedback and review of this document. I would also like to extend them my sincere gratitude for being a part of my committee.

I would like to show appreciation to my colleagues at the Photovoltaic Reliability Laboratory at Arizona State University (ASU-PRL) for their help and interest in the project. Special thanks to Lorenzo Tyler, Faraz Ebneali, Sai Tatapudi and Kolapo Olakonu for their help during the project.

Lastly I would like to recognize the importance of the Photovoltaic Reliability Laboratory facility at Arizona State University in providing a great learning environment in which these types of experiments can be conducted.

TABLE OF CONTENT

Page

CHAPTER Page

CHAPTER Page

Page

LIST OF TABLES

Table Page

LIST OF FIGURES

Figure Page

Figure Page

Figure Page

CHAPTER 1

INTRODUCTION

1.1 Background

Several climatic factors affect the performance of PV modules in outdoor applications. Conditions such as Irradiance, humidity, soiling, high ambient temperatures and others contribute to module degradation over its lifetime. However, PV modules tend to be stressed and affected most from high temperature generated due to irradiance from sun. Highest power and energy losses are due to the high operating temperatures experienced by a module and the overall system. Solar cells have a power temperature coefficient of -0.5% for every 1ºC rise in temperature. The power rating of a solar module is performed at Standard Test Conditions (STC) of 1000 W/m^2, 25ºC and AM of 1.5. It is common for a PV module to reach temperature of 45 to 65 ºC (20-40ºC above STC) which leads to power drop in the range of 10-20%. Additionally, during the summer months, building applied photovoltaic (BAPV) installation in desert climatic conditions such as Mesa, Arizona may experience module temperatures of up to 85ºC. This may lead to performance drop of up to 30%. As a result, systems will have a significant drop in AC power output when derated due to wire, voltage drop, soiling and inverter losses which would then lead to a significant loss in energy output for the year.

With the current state of federal and government incentive programs and solar becoming cheaper and cheaper day by day, Industry is primarily concerned with ensuring the maximum system output (kWh/kWp) and longer system lifetime, since the longer the lifetime, the longer the energy output for the installed system. The cost, referred to as ($/kWh) of the total kWh produced from a

system on an annual basis can be lowered as a system experiences lower losses (greater production). With primary concerns of improving system throughput, industries are now looking into making use of the thermal energy/heat to compensate for array losses.

Traditionally system Integrators usually opted for a suitable air gap to allow for ventilation which would channel for the hot air underneath to escape and allow for some cooling. The size of the air gap determined module operating temperature, which in turn lead to determining performance [1]. This led to the Master's thesis by Jaewon Oh at Arizona State University where temperature data was monitored and collected over a year for BAPV modules installed with various air gap sizes (0, 1, 2,3 and 4 inches) [1] . Oh's study recommended 3 inches air gap to be the most suitable air gap in terms of performance. However his study consisted of four different module types from four different manufacturers. This study was later continued by another masters student, Ben Schams[2] where he implemented multiple modules of the same type for developing his mathematical models and by ensuring the same set of air gaps.

The effect of ambient conditions on a large continuous array with multiple modules of the same type installed at a consistent air gap was studied by Jonathan Hrica in his thesis [3]. Jonathan also introduced a small fan to understand the effects of array level cooling in his work.

However till now a side-by-side identical array analysis with identical air gap was not conducted to help better understand the effects of fan cooling and array performance under similar ambient conditions. Having two side-by-side BAPV arrays helped keep one system as control array and the other system as a test

array. Test array was constantly evaluated with varying configurations such as fan without wind blocks (Configuration II), Fan with wind blocks on top and sides (Configuration III) and fan with wind blocks on top, sides and bottom of array (Configuration IV). Test Array for Baseline setup was designated as (Configuration I)

1.2 Statement of Purpose

In a previous study [3], the effect of fan cooling was investigated consecutively (fan ON for a period of time and fan OFF for the consecutive period of time) on a single array under varied ambient conditions. In this study, the effect of fan cooling has been investigated simultaneously on two arrays (control array without fan and test array with continuously running fan) under identical ambient conditions. The idea here is to reduce module operating temperatures and help improve temperature uniformity and performance.

1.3 Scope of Project

The project included set up of following tasks:

- Baseline current-voltage characterization of 24 polycrystalline-Si Photowatt modules
- Installation of 24 modules at an 3-inch air gap from the rooftop
- Installation of 36, type-K thermocouples for module, air gap, tile as well as inside roof temperatures.
- Installation of Vaisala WXT weather station to monitor wind speed, direction, ambient temperature, rainfall, atmospheric pressure and relative humidity.
- Installation of EETS calibrated reference cell and EKO MS-602 pyranometer to measure plane of array global irradiance

- Design and installation of fan cooling system to act as exhaust
- Programming of Campbell Scientific CR-1000 data acquisition system with AM 16/32 Multiplexer.
- Data collection with and without wind blocks at various stages: top wind block; top and side wind block; top, side and bottom wind block
- Current voltage measurements of rooftop installed modules at row-level (2 modules in series) and array-level (12 modules in series)
- IR imaging of array under all four configuration using Fluke IR camera
- Data processing and analysis for fan cooling effect on temperature uniformity and performance improvement
- Development of Thermal models

1.4 Assumptions

Several assumptions are considered in this project moving ahead. To be non-intrusive, the thermocouples are attached to the back of the modules for monitoring cell temperature. As a result the temperature measured will be about 1.5^{o}C lower than the actual cell temperature. At the same time, the tip of the thermocouple is attached to the centermost cell, considered to be the representative part of the module temperature.

1.5 Limitations

Thermal models developed in this work will help predict module temperature based on a set of ambient conditions. However, these models are only validated for Mesa, AZ and may or may not be applicable for conditions outside Mesa. Also, the temperature readings of the modules were taken under open circuit conditions. The temperature readings of modules under load might be slightly different.

CHAPTER 2

LITERATURE REVIEW

2.1 PV Module Temperatures

The active circuit (cells) is encapsulated in a module for safety, durability and reliability. The encapsulation leads to alteration in heat flow in and out of PV module, thereby increasing the operating temperature. Module Temperature is typically understood as equilibrium developed due to [4]

- Heat generated from module due to irradiance
- Heat lost to surrounding from the module (methods described later)
- Ambient air temperature

Although high temperatures slightly help increase short circuit current (Isc), but leads to a much higher drop in open circuit voltage eventually leading to an overall drop in module power. High module temperatures are also associated with accelerated failure mechanisms which lead to module degradation and reduction in array lifetime. As well known Arrhenius Law indicates, for the typical thermal failure mechanisms the module lifetime is typically expected to halve for every 10˚ C rise in temperature. Module operating temperature is typically determined once the module is in a state of thermal equilibrium, defined as the net temperature between the heat produced from the module itself, ambient temperature and heat lost to the environment.

PV modules typically convert only about 14-20% of the incident solar irradiance into useful electrical energy. The rest of the sun's energy incident is mostly converted (~75%) into heat. Primary factors piloting the effect of heat buildup in a PV module are [5]:

- Operating point and efficiency of a PV module
    - If a module is operating in its maximum power point region, then the incident irradiance is utilized for electricity production. However if the module is in Isc or Voc, then all power absorbed by the cell is converted to heat.
- Absorption of light
    - Absorption of light by parts of a module other than cell, would dissipate heat and contribute to heating of module. At the same time, the heating properties would also depend on material composition of the PV module.
- Absorption of Infra-Red light
    - For photons to contribute to electron hole pair, the energy of the photon must be equal to the energy of the band gap. If the energy of the incident photons is less, it might be absorbed by the module and contribute to heating.
- Packing Factor of the Solar Cells
    - Cells are closely packed together to reduce series resistance and be more efficient absorbent of incident solar irradiance. However a higher packing density also leads to higher generate heat per unit area.

2.2 Heat Loss Mechanisms

For BAPV systems having smaller air gaps, it is essential for the modules to employ mechanisms to mitigate heat loss for efficient light to electrical conversions [6].

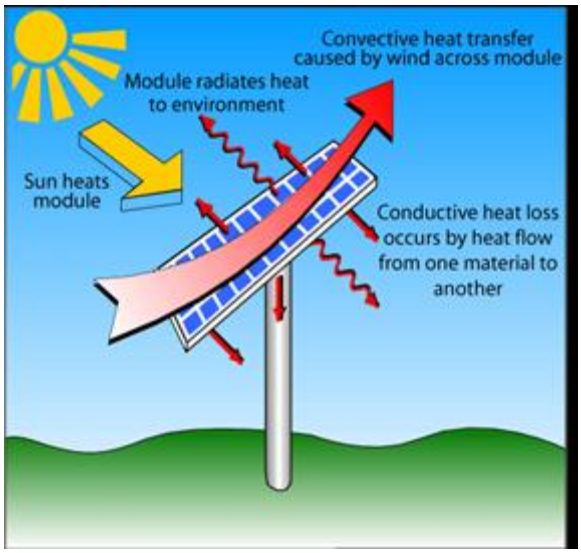

Fig 2.1 Conduction, Convection & Radiation heat losses [6]

2.2.1 Conduction

This thesis focuses on a side by side BAPV system installed at a consistent air gap of 3 inches from the rooftop. Typical methods of conductive heat looses for BAPV systems would result due to development of a thermal gradient between the module and surrounding air temperature. The higher the difference in the temperatures, the greater the heat flow from the module. However, the heat flow from the module is also proportional to thermal resistance, a material property such as encapsulant type surrounding the active area. This may be described in the form of a mathematical equation as shown below in Equation (2.1) [6]:

$$\Delta T = \Phi P_{heat} \quad (2.1)$$

Where

ΔT = Temperature difference between two materials in ^{o}C

Φ = Thermal resistance of emitting surface in $^{o}C\ W^{-1}$

P_{heat} = Heat generated by the PV module

2.2.2 Convection

Convection heat loss from a module is mainly due to the effect of wind blowing over the surface of the system under consideration [6]. Typically wind tends to carry heat from one point to another, as it comes in contact with the surface. The process can be more elaborated through the Equation (2.2) as follows [6]:

$$P_{heat} = hA\Delta T \quad (2.2)$$

Where:

A = Area of contact between two materials

h = convection heat transfer co-efficient, ($W/m^2/^oC$)

ΔT= Temperature difference between two materials ($^\circ C$)

2.2.3 Radiation

The third and final method of dissipating heat to the surrounding by a PV module is by means of radiation. Typical BAPV systems employing lower roof air gaps would conduct heat into the air gap, which would be radiated into the building [6] This can be mathematically explained using Equation (2.3) as follows [6]:

$$P = \epsilon\sigma(T^4_{SC} - T^4_{amb}) \quad (2.3)$$

Where:

T_{sc}= Temperature of Solar cell (^oC)

T_{amb} = Temperature of the ambient surrounding the solar cell (^oC)

σ = Stefan-Boltzmann constant ($5.67x10^{-8}\ J/m^2sK^4$)

ϵ = Emissivity of the surface (0.03)

2.3 Temperature Coefficients

A module is rated at standard test conditions (STC) which lists the electrical parameters of the module at 1000 W/m^2, 25^oC and AM 1.5. However, in real world conditions, modules easily surpass such conditions. In order to evaluate

the electrical parameters due to the changes in temperature, temperature coefficient values are used. Temperature coefficients are means of determining the effect of temperature on module Power (Pmax), Open Circuit Voltage (V_{oc}) and Short Circuit Current (I_{sc}). Every module manufacturer has temperature coefficients listed in the module specification sheet. When designing systems, NEC or National Electrical Code states multipliers to derate for site specific ambient temperature. At the same time, it emphasizes to use manufactures provided temperature coefficient values to calculate for source open circuit voltage as a safety criteria.

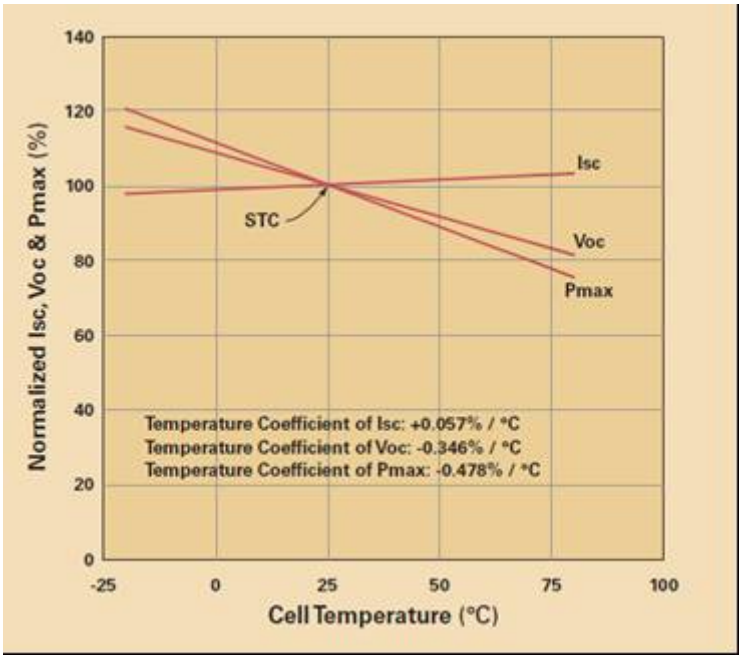

Figure 2.2 Temperature Coefficients [3]

The graph above lists the three critical temperature coefficients necessary to evaluate the effect of temperature on cell characteristics. As it can be clearly seen from above, an increase in temperature leads to a slight increase in short circuit current (Isc), whereas an increase in cell temperature is leading to a drop

in both open circuit voltage (Voc) and power at maximum power point (Pmax). It is also important to note that, even though there is an increase in Isc with the change in temperature, the gradient for change in Voc is much steeper, contributing to the overall loss in cell power.

2.4 Effect of ambient conditions

The discussion of this paper has been focused on the cause of high temperature origination [4] in a PV module and mechanisms through which a certain PV module may dissipate heat to surrounding conditions and temperature related issues with PV modules [6]. However, together with high operating temperatures, ambient conditions such as irradiance, soiling, wind speed, humidity and proximity to rooftop (air gap) tend to contribute to module degradation over its lifetime as well. Thermal modeling may be adopted as a mathematical procedure to predict module temperature based on several ambient conditions. Multiple thermal models are fabricated as well as evaluated in this study to predict the temperature of a module/array at a known site with collected ambient condition data.

2.5 Thermal Models

PV cell or module when placed in field conditions undergoes various environmental stresses such as humidity, wind speed, ambient temperature, soiling, air gap temperature effect and so on. All of the stresses have an implication on the module temperature which must be understood. Thermal models are developed which help predict module temperature based on climatic factors. For our study, wind speed, irradiance and ambient temperature are considered.

2.5.1 Sandia Thermal Model (Simple Model)

When designing a PV system, it is essential to understand its thermal properties to predict annual energy production. An empirical based thermal model (Simple Model) had been recently developed at Sandia [7].

The model is described in Equation (2.4) [7]:

$$T_m = E \cdot \{ e^{a+b \cdot WS} \} + T_a \quad (2.4)$$

Where:

Tm = Back Surface Module Temperature, (ºC)

Ta = Ambient Air Temperature, (ºC)

E = Solar Irradiance Incident on Module Surface, (W/m^2)

WS = Wind speed measured at standard 10-m height, (m/s)

a = Empirically-determined coefficient establishing the upper limit for module temperature at low wind speeds and high solar irradiance

b = Empirically-determined coefficient establishing the rate at which module temperature drops as wind speed increases

The coefficients determined in the model are obtained using an array of temperature measurements recorded over several different days with the module operating in a near thermal equilibrium condition. Thermal equilibrium is achieved by measurement on consistent sunny days without intermittent cloud cover. The simple model has proven to be adaptable and entirely adequate for system engineering and design purposes with an accuracy of +/-5ºC [7].

2.5.2 Cell Temperature Prediction

Typically cell temperature is relatively higher than module temperature. The temperature of the cell inside the module can be related to the module back surface temperature through a simple relationship provided in Equation (2.5) [7]:

$T_c = T_m + [E/E_o] \cdot \Delta T$ (2.5)

Where:

T_c = Cell Temperature inside module, (ºC)

T_m = Measured back surface module temperature, (ºC)

E = Measured Solar irradiance on module, (W/m^2)

E_o = Reference Solar Irradiance on module, (1000 W/m^2)

ΔT = Temperature difference between the cell and the module at an Irradiance level of 1000 W/m^2

2.5.3 Nominal Operating Cell Temperature (NOCT)

Nominal Operating Cell Temperature can be described as the predicted temperature of the module under the ambient conditions of irradiance at 800 W/m^2, ambient temperature of 20 (ºC) and wind speed less than 1 m/s. The wind speed model can be described as shown below in Equation (2.6) [8]

Tc = TA + [[(NOCT-20)]/0.8]*G (2.6)

Tc = Module Predicted Cell Temperature

TA = Ambient Temperature (ºC)

NOCT= Module NOCT value (ºC)

G= Irradiance (kW/m^2)

The NOCT value may be obtained from the module specification sheet at the back of the module, provided by every manufacturer.

2.5.4 ASU PTL model

Extensive field work has been performed at Arizona State University, Polytechnic campus to develop thermal models for both open rack as well as rooftop applications. One of the initial thermal models which employed irradiance, wind speed, relative humidity, ambient temperature and wind direction was developed

in conjunction with NREL laboratory. Temperature data were collected on multiple modules at both sites for a period of 2 years from 2000 to 2002. Ambient weather conditions were also monitored. Once the data had been collected, Matlab neural network was used to calculate the value of the coefficients and validate the thermal model which is detailed in Equation (2.7) [9]

Tmodule = w1 * Tambient + w2 * E + w3 * WindSpd + w4 * WindDir + w5 * Humidity + C (2.7)

Where:

Tmodule = Module Temperature (ºC)

Tambient = Ambient temperature (ºC)

E = Measured Irradiance (W/m^2)

WindSpd = Wind Speed (m/s)

WindDir = Wind direction (º)

Humidity = Relative humidity (%)

C = Constant

(w1~w5): Derived Coefficients

The above thermal model has since then been revised to consider for only three parameters such as irradiance, wind speed and ambient temperature and is provided below in Equation (2.8) [9]

Tmodule= w1 * Tambient + w2 * E + w3 * WindSpd + C (2.8)

Thorough regression analysis on ambient data collected and using both equations discovered the three parameter equation to be more accurate and suitable especially for Mesa Arizona conditions. The last two environmental conditions (WD & RH) showed minimum or negligible impact on module temperature and instead introduced more deviation with the coefficients. The

three parameter equation was first developed and tested on an open rack array configuration by a Master's thesis titled, "Outdoor Energy Rating Measurements of Photovoltaic Modules of Photovoltaic Modules" by Yingtang Tang [9]. This thermal model was based on open rack with resistive loading. Radhika Lad, another Masters student implemented the identical thermal model with MPPT loading[10]. Her work incorporated both Yingtang Tang and Sandia's approach. The same model was later adopted for short-term (one month) roof mounted array for Master's thesis called, "Temperature of Rooftop Modules: Effect of Air Gap and Ambient Condition" by Bijay Lal Shreshtha[11]. Later on a long term (one year) study of this thermal model was executed in a study named, "Building Applied and Back Insulated Photovoltaic Modules: Thermal Models" by Jaewon Oh [1]. This work was continued further using identical modules in a Master's thesis titled, "Effect of Air Gap on Building Applied Photovoltaic Modules: An Energy & Economic Analysis" [2]

Much recently the three parameter thermal model has been applied towards understanding the effect of ambient conditions and fan cooling on a single air gap installed 1.2 kW system. The results of such study are documented in thesis titled, "BAPV Thermal Modeling and Fan Cooling" [3].

Finally, this present thesis analyzes the three parameter thermal model at two side-by-side arrays, installed at single air gap with several modules of same type.

2.6 Photovoltaic Thermal Systems Concept (PV/T)

PV/T air or PVT/Air systems can be considered as an efficient and cost effective alternative to BAPV systems [12]. A PVT/Air system is easy to construct and operate mainly as the concept is based on channeling the hot ambient air out from underneath the system to mitigate system losses and help improve

electrical efficiency. At the same time, the PVT/Air system is also helping contribute to thermal gain, such as residential heating and cooling. In common rooftop BAPV applications, high PV operating temperatures are radiated into undesirable heat transfer to the building, mainly during summer [12]. For such applications PVT/Air systems with air channels would exhaust hot ambient air out from underneath the system and help achieve both PV cooling and thermal energy output, which may be used for building thermal needs. EchoFirst Inc from California, USA is already having the technology in industrial application. The company is channeling the hot stagnant heat from underneath the solar array for residential space heating and air conditioning purposes [13]. The necessary pump, heat exchanger, and pipes for air circulation constitute the entire system and bring the heat to its eventual use.

This paper explores the concept and results from a proof of concept PVT/air system. The system employs a 40 Watt exhaust fan and aluminum ducts which are designed to act as channels to exhaust the hot ambient air from underneath the system. The fan has been kept on throughout the study to understand cooling on the test array as compared with control array.

CHAPTER 3

METHODOLOGY

3.1 Site Description

The project is being conducted at Photovoltaic Reliability Laboratory (PRL) outdoor field testing area. PRL is located at Arizona State University - Polytechnic campus which is east of Phoenix, Arizona. The goal of the project is to understand the effect of fan with ambient conditions on two side by side small scale photovoltaic arrays (Control & Test). As a result, the pitch of the mock rooftop was determined to depict real world residential rooftops (23º). Also, the site is clear of any obstructions such as light poles or trees that would create any form of shading which might hinder performance. This project incorporated a tuff shed as a mock rooftop which used wooden frames, insulation and other materials typical in a residential construction. The tuff shed is south facing and measures 33 feet by 17.5 feet.

3.2 PV array installation

This thesis is a study of two side by side arrays. The installed arrays consist of 12 poly c-Si modules each at an air gap spacing of 3 inches from roof surface to the bottom of the frame. The characteristics of the modules are provided as follows:

- Test technology: poly c-Si modules
- Manufacturer: PhotoWatt
- Number of modules: 24 (12 each)
- Electrical termination: Modules under open circuit (no load)

Both arrays are laid in the pattern of 6 rows x 2 columns. The rows and columns have one inch spacing between them to allow for thermal expansion and

contraction during high temperature days. The modules are arranged in landscape orientation (horizontal) supported by long metal rails. The rails are attached to the roof trusses at various attachment points using L brackets and hex bolts.

Since the bolts are penetrated to the rooftop, a roof sealant has been applied at every attachment point to ensure safety from water leakage during monsoon seasons and to keep the equipment inside the building safe from any water damage. A walkway of 3 ft between the arrays has been implemented to allow better accessibility to modules on top row and other instruments and to ensure that the test array heat or control array heat is not influencing the other array depending on wind direction.

Figure 3.1 below shows a snapshot of arrays installed side by side on the mock rooftop.

Figure 3.1 Side-by-Side PV Array

This thesis further explores the implementation of a fan system and wood blocks in array ventilation and cooling. The setup and results are discussed in detail later on as we move into chapter 4 of the thesis.

3.3 Module Preparation

Poly c-Si modules have been chosen as the technology for analysis during this study. The electrical specifications for the modules are provided in the table below in Table 3.1:

Table 3.1: Module Electrical Characteristics:

Manufacturer	Electrical Specification				
PhotoWatt	Voc(V)	Isc (A)	Imp(A)	Vmp(V)	Pmp(W)
	43.2	2.9	2.8	34	95

A single cell from each module was selected for temperature measurement. In making the selection for the cell, it was ensured to select the centermost cell as the temperature monitoring cell, as it tends to get the hottest.

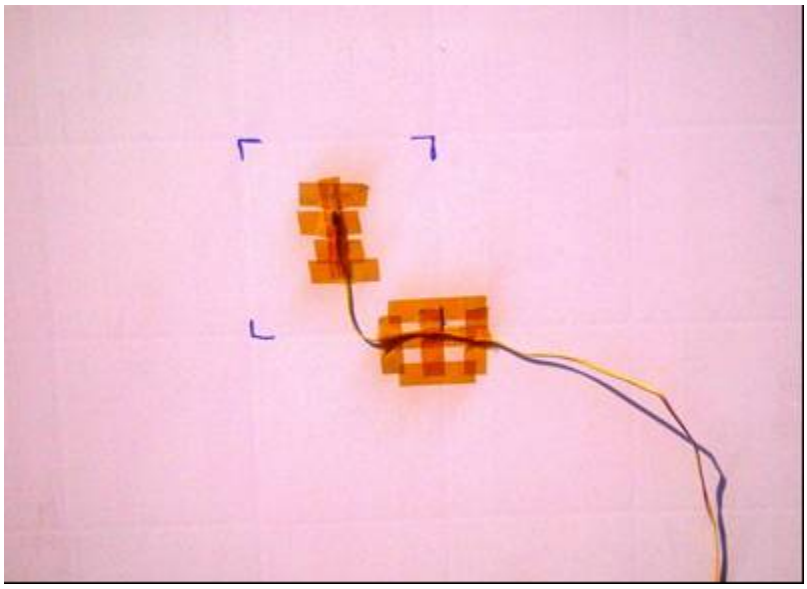

Figure 3.2 Thermocouple Attachment point

Every individual module was rewired as the PV wires that the modules came attached with were short and introduced a significant issue since part of this study required connecting the entire array in series for I-V curves to be obtained.

The images for the rewiring of the modules are provided below in Figure 3.3

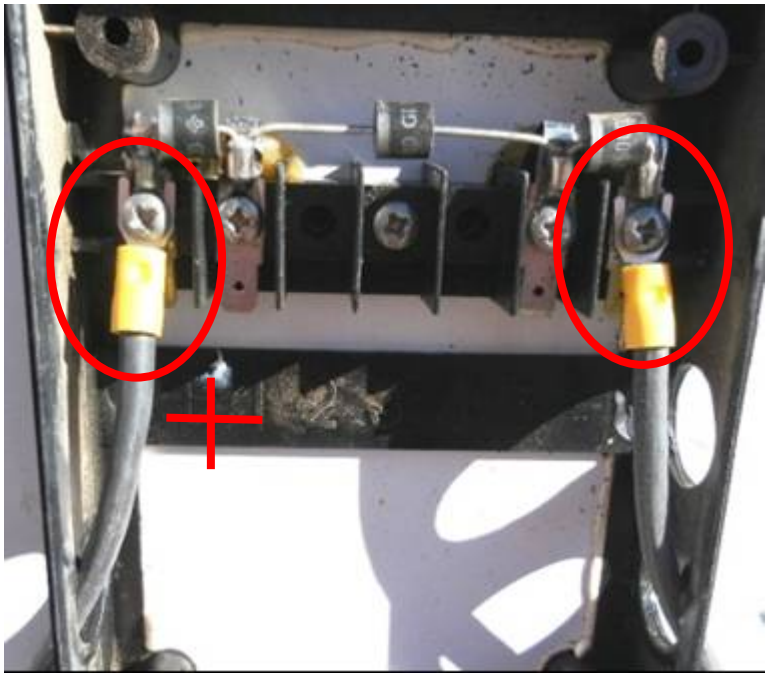

Figure 3.3 PV wire terminal wiring

Standard 10 AWG industrial grade UV protected PV wire of equal length was attached to the terminals and tested for connection as shown in Figure 3.4

Figure 3.4 Completed wiring

Due to the age of the modules and previous wear and tear, some of the junction boxes attached to the back of the modules lacked proper insulation. Since the proximity to rooftop for the panels was only three inches, this provided severe electric danger and possibility of arcing during occasional monsoons, if water would penetrate through the opening in the junction box.

The use of insulating foam sealant ensured that the gaps and cracks in the junction box were sealed to avoid any unwanted condensation or water.

3.4 Ambient data

Ambient conditions such as wind speed, wind direction, temperature and irradiance along with several other parameters are continuously monitored. Irradiance measurement devices are installed on the same roof as the array, ensuring the devices maintained the same plane of the array during the measurement (POA). EETS calibrated reference cell and EKO-MS 602 pyranometer measured irradiance where the reference cell measurements have been used as the primary data. Vaisala WX520 Weather station provided values for wind speed, humidity, ambient air temperature, rainfall and air pressure. RM young wind speed and direction sensor provided the respective wind speed and direction as well. In this case, data from RM young has been considered to be the primary data source. Collected data such as wind speed, irradiance and ambient temperature is then used for the Matlab based thermal modeling in this thesis. Figure 3.5 below shows the devices installed on the rooftop.

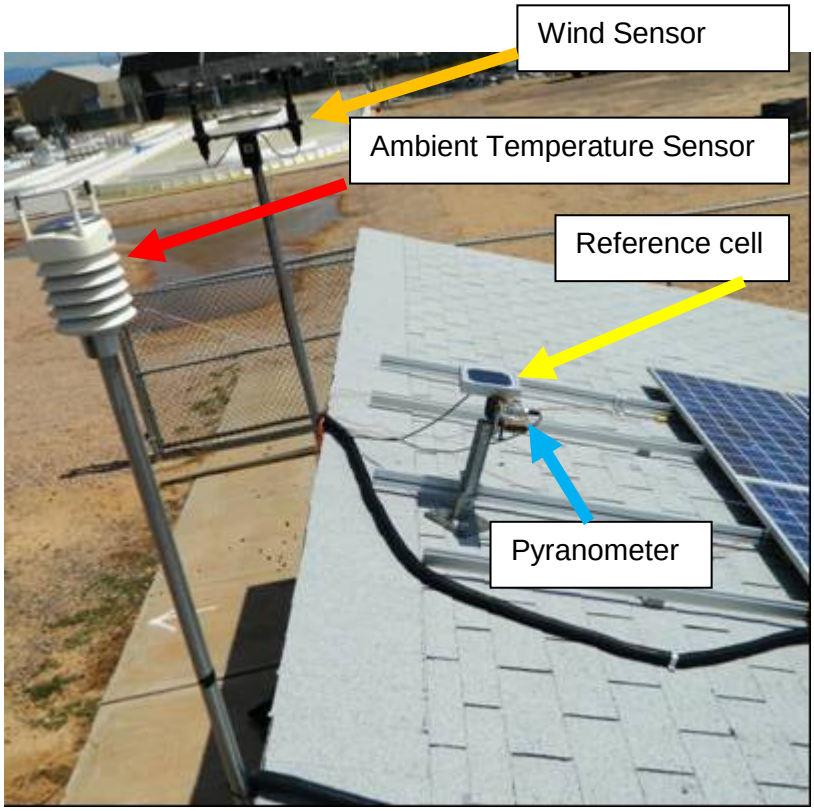

Figure 3.5 Ambient data measurement equipment

3.5 CR 1000 Installation

This thesis incorporates the use of a Campbell scientific CR 1000 datalogger in conjunction with AM 16/32 multiplexer as the data acquisition system (DAS) for the project. The multiplexer features extra analog channels for expansion capability which were then used to connect to devices such as thermocouples extending from panels. This thesis is a combination of devices such as thirty-five thermocouples for measuring module, air gap and tile temperatures respectively. CR 1000 was set up and programmed to collect data from each instrument at regular intervals of one minute. The data was then averaged every six minute and stored in CR 1000's memory. However with limited options available at CR 1000 such as only 16 analog channels, an AM16/32 expansion multiplexer was used to retrieve data from the remaining devices.

The initial goal of the project was to house the DAS in a casing attached to the outside of the north facing wall of the shed. Later on, as that provided a possibility of some damage due to dust storm and occasional monsoon, it was quickly decided to house the DAS inside the building on a wooden board as shown in image 3.6

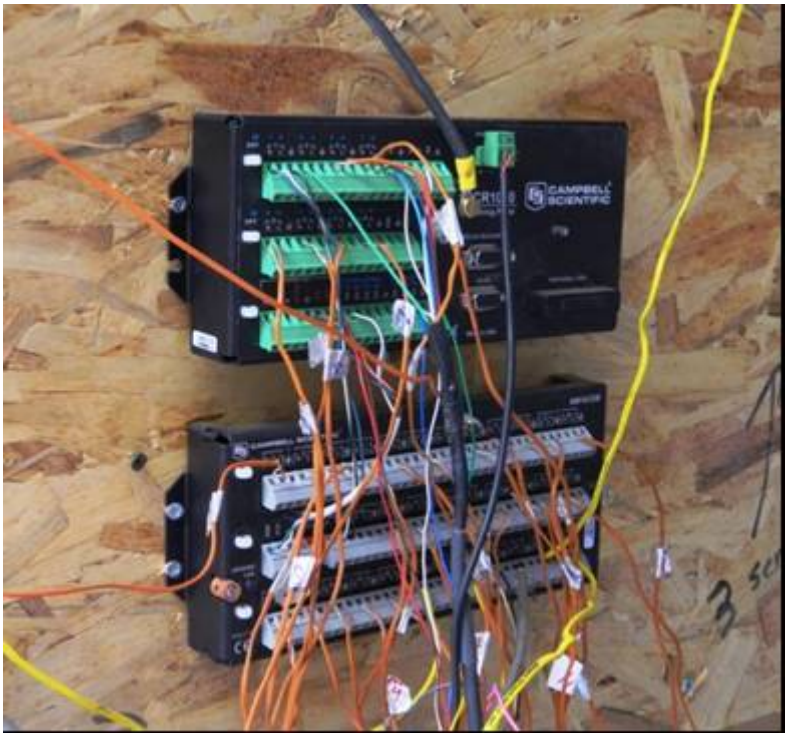

Figure 3.6 DAS & Multiplexer inside Tuff shed

The CR 1000 has been grounded as shown in image to protect the device from any potential voltage transient due to occasional power surges.

3.6 CR1000 Programming

Campbell Scientific CR 1000 has an easy to use menu driven software (Short Cut) which can create customized programs for particular applications. Short Cut is a programming wizard available for CR 1000. Short Cut can be accessed through PC 200, a CR 1000 support software as shown in image below.

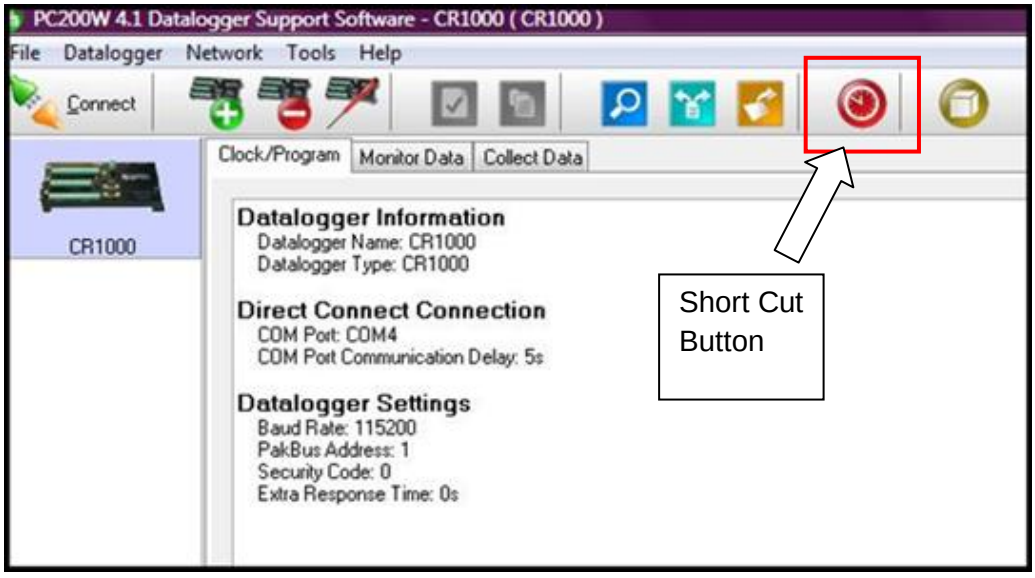

Figure 3.7 Short Cut Button in PC 200

Once the shortcut window opens, we can create or open a saved program, select the respective sensors, select the type of outputs and then send the program to the data logger. The selections made using Short Cut program are designed to tell CR 1000 what devices are connected to it and how often to fetch information from them. The user may also program Short Cut to retrieve data in the form of averaged or sample collection. Figures 3.8 and 3.9 show the standard sequence of device selection and CR 1000 connection.

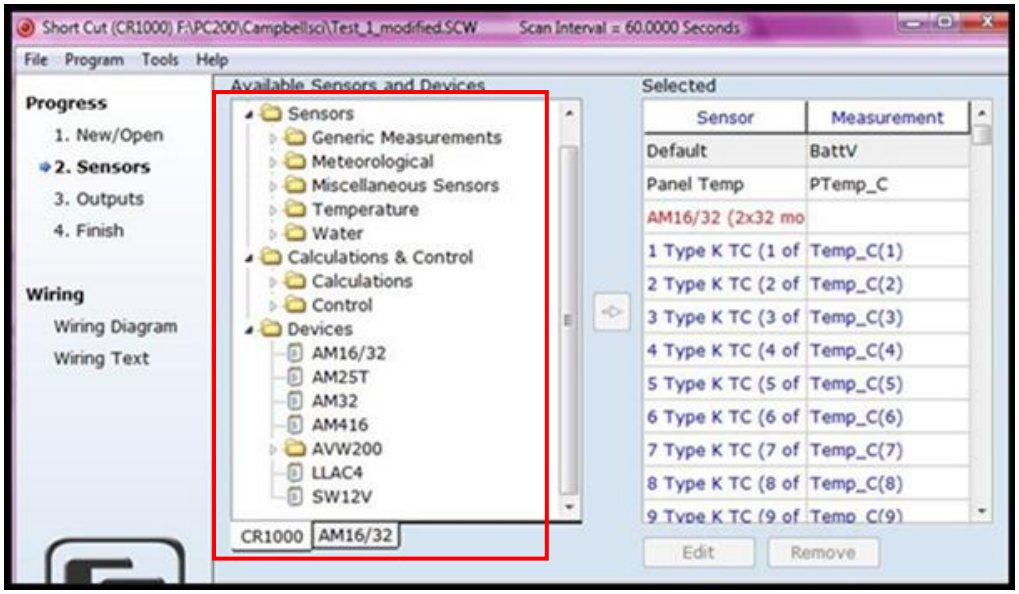

Figure 3.8 Sensor Selection

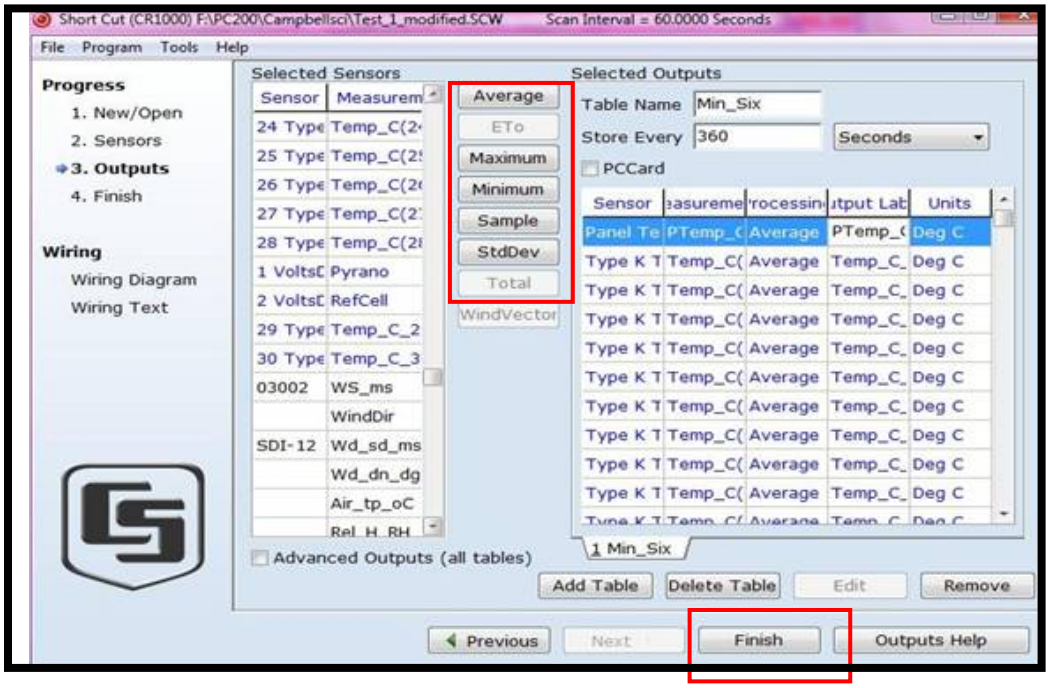

Figure 3.9 Final Selection and Send

Once the program knows the devices to be connected, it generates a wiring diagram which must be followed for connection to the CR 1000 data logger, as failure to do so would not allow the data logger to function. An image of the wiring

schematic is shown below in Figure 3.10

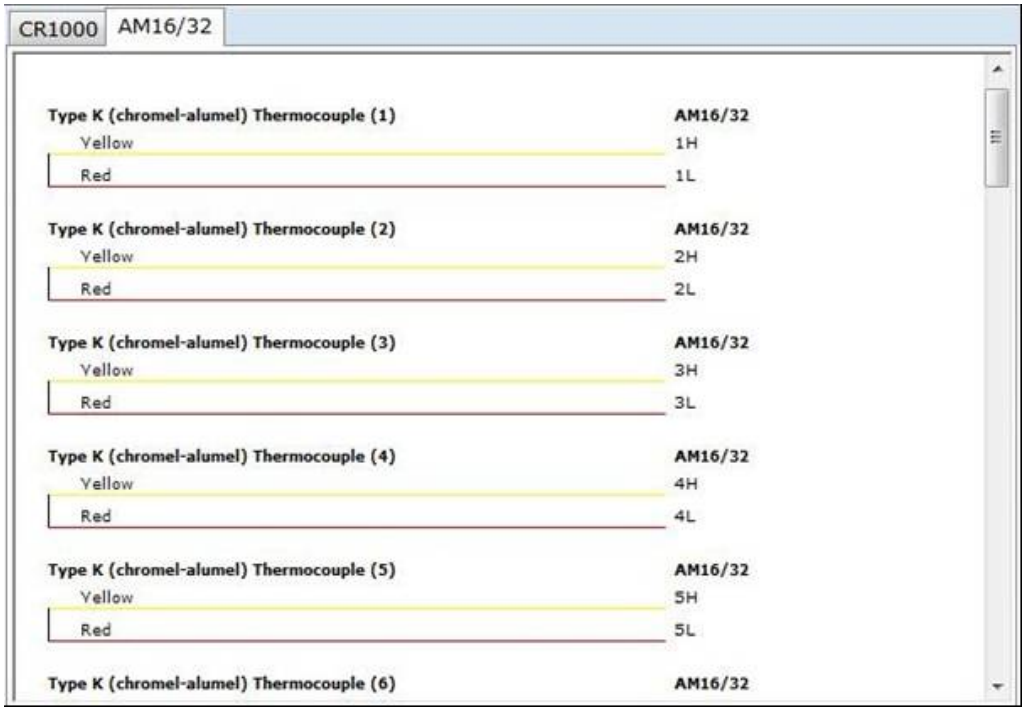

3.10 Wire Connection Wiring Diagram

3.6.1 CR 1000 Data Download

As mentioned earlier in the document PC 200 is a support software for CR 1000. It provides an option to either monitor the data or collect data once a connection has been acquired with the CR 1000. For ex. monitoring the data is always advisable to ensure that there are no faulty thermocouple readings before the data is downloaded. The tab to monitor and collect data is shown below:

Figure 3.11 Data Download Image

Once collected, the data can be copied and edited in excel. This thesis explores the data for use in thermal modeling, effect of array temperature uniformity under various wind speed, wind direction and irradiance conditions. The data is simply downloaded by establishing a connection with a laptop computer using an RS-232 cable when required.

3.7 Fan Cooling System

Since this thesis is an analysis of fan cooling on side by side systems, the aim of this segment of the project was to understand if the ventilation effect from the fan helped mitigate high temperature losses in one system compared to another. Since both systems were under similar ambient conditions, it provided an excillent opportunity to introduce a study of such sort.

This study is an extenstion from another Masters student work, Jonathan Hrica thesis titled, “ BAPV Analysis: Thermal Modeling & fan Cooling”. However the study on his thesis was only based on one system, so changing from fan and no fan condtions introduced variations in ambient conditions. The fan size was based on power rating and typical power losses experienced from this system installed on the mock rooftop. The array installed on the rooftop is DC rated at 1140 Watts, under standard test conditions. During high operating temperatures, this array might experience power losses of upto 20%, leading to 228 Watts. Thus a fan with power consumption more than this would not have been feasible. The current fan under operation is rated at 40 Watts, a small consumption. The fan of such sort is rated for high temperature operation and is typically used as a booster fan for residential HVAC. The fan assembly is attached to multiple 6 inch diameter aluminum ducts which act as exhaust to pull air from bottom to top of the array eventually pushing the air out. The fan is housed in an 8 inch diameter

ducting. All material is constructed out of aluminium, to ensure there is no leakage. Meanwhile any gaps or holes are sealed from UV protected tape. Figure 3.12 depicts the fan setup used in the project.

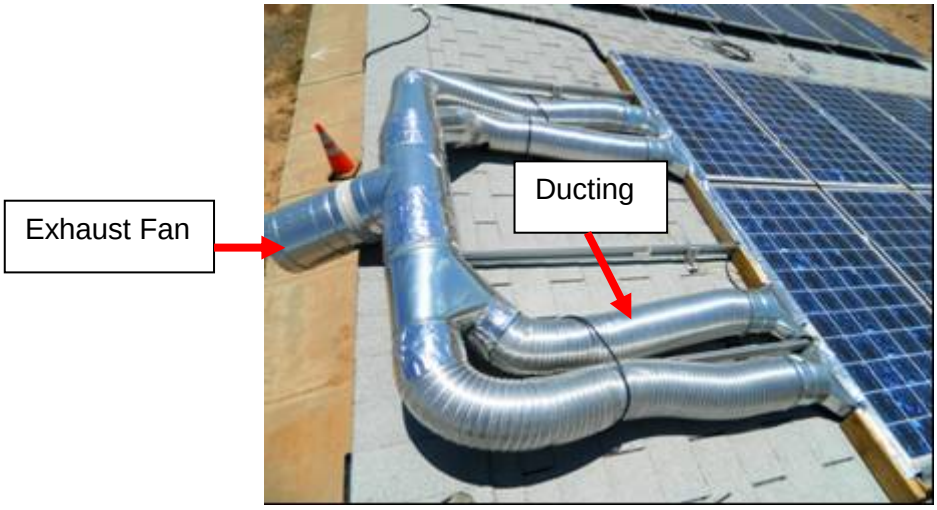

3.12 Fan with Aluminium Ducting

3.8 I-V curves

3.8.1 Row level I-V curves

This thesis explores system performance analysis in two parts. The first part of the thesis looked into collecting three I-V curves for every single row of the array. The protocol was executed at one selected day under similar amibient conditions for all four stages including baseline. This helped determine inter-row performance going from top to bottom for both side by side systems.

3.8.2 Array level I-V curves

Later on to introduce more accuracy, the entire array was connected in series and an I-V curve was obtained. For both side-by side systems, it was ensured that the I-V curves between both systems are taken within 5 mins to prevent shifts in ambient conditions such as Irradiance. Figure 3.13 shows the schematic for entire array connection.

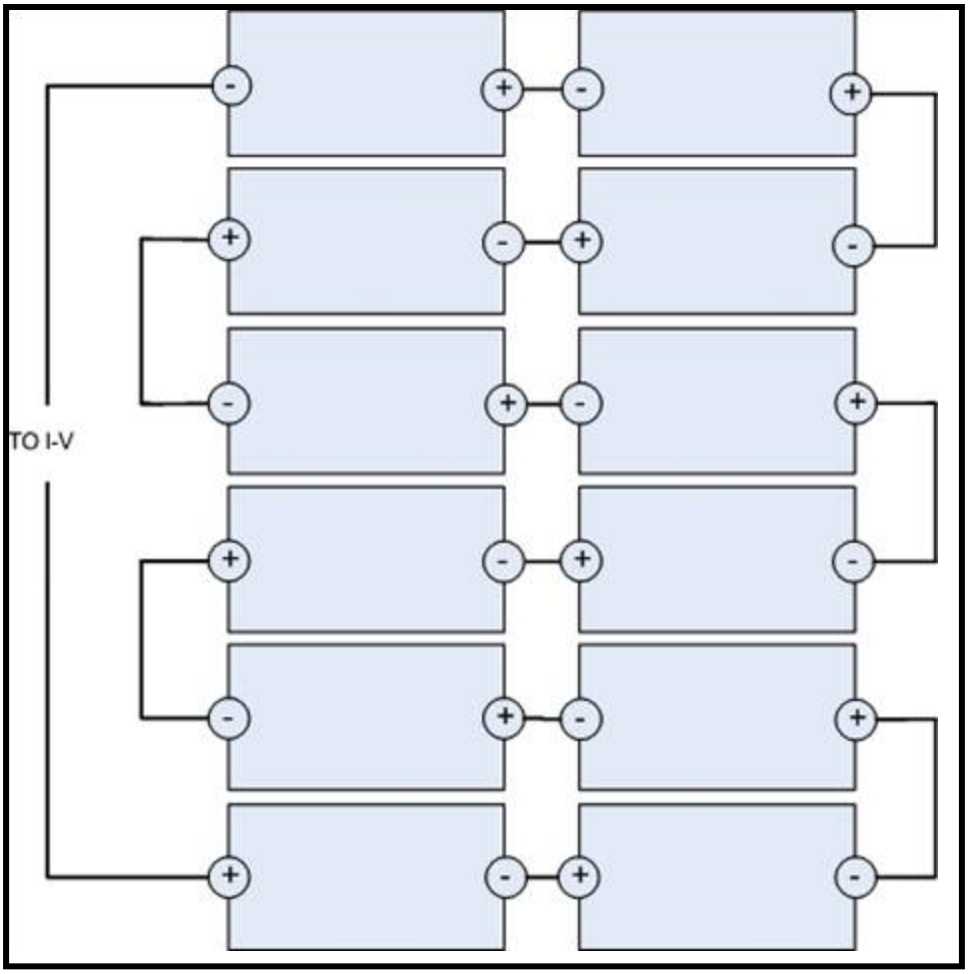

3.13 Test Array Series Connection for I-V

3.9 Infrared imaging (IR)

Last segment of this thesis looked into IR imaging for all four configurations. IR images were obtained using the IR Flexcam Fluke Thermal Imager camera (Ti-55) in the outdoor field facility at PRL. For better imaging the modules/panels had to be electrically short ciruited before we proceeded with any images. For this reason the entire array was shorted. However, due to the nature of high voltage associated with the arrays (518 V each) the arrays were covered with industrial grade tarp during the day while dealing with any elecrical connections. . Once the electrical connections were made, tarps were removed and system was left in shorted condition under sun for 15-20 mins to reach thermal equilibrium,

before an image was attempted. Figure 3.14 shows both side by side systems under tarp

3.14 System covered in tarp for pre-IV connections

The results and analysis of the IR images are discussed in detail in chapter 4 of this thesis.

CHAPTER 4

RESULTS & DISCUSSION

4.1 Side by Side Thermocouple Spot Check

BAPV systems typically operate at higher temperatures due to close proximity from the rooftop. High temperature operation has a negative effect on the module electrical performance such as voltage and power and eventually lifetime. For this study a Campbell scientific data acquisition system (DAS) has been installed and programmed to document module temperatures at regular intervals. The module temperature is fed into the DAS by use of K-type thermocouples which are attached to the backsheet of the modules. A quick check at noon conditions on June 22nd was performed to verify if similar temperature distribution was observed along test and control array. The result of the test are shown below

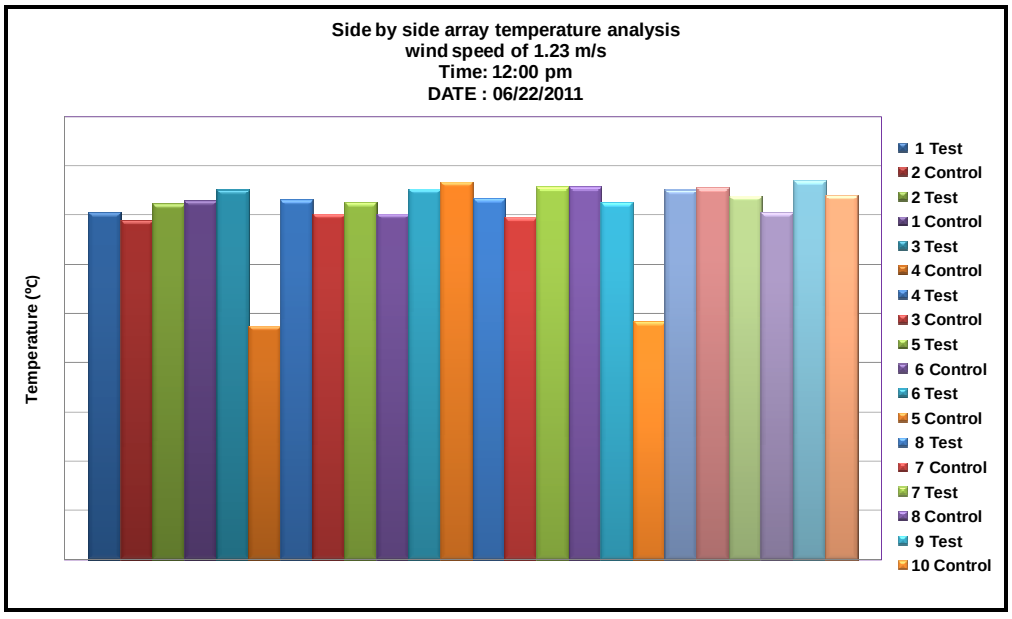

Figure 4.1 Temperature Pattern Check and Thermocouple Validity Analysis

As it is noticed above from Figure 4.1, from this initial check two thermocouples were registered to be defective. The defective thermocouples were later removed, tested with a multimeter and opened to conclude a short inside the thermocouple which recorded such low values.

4.2 Temperature Analysis

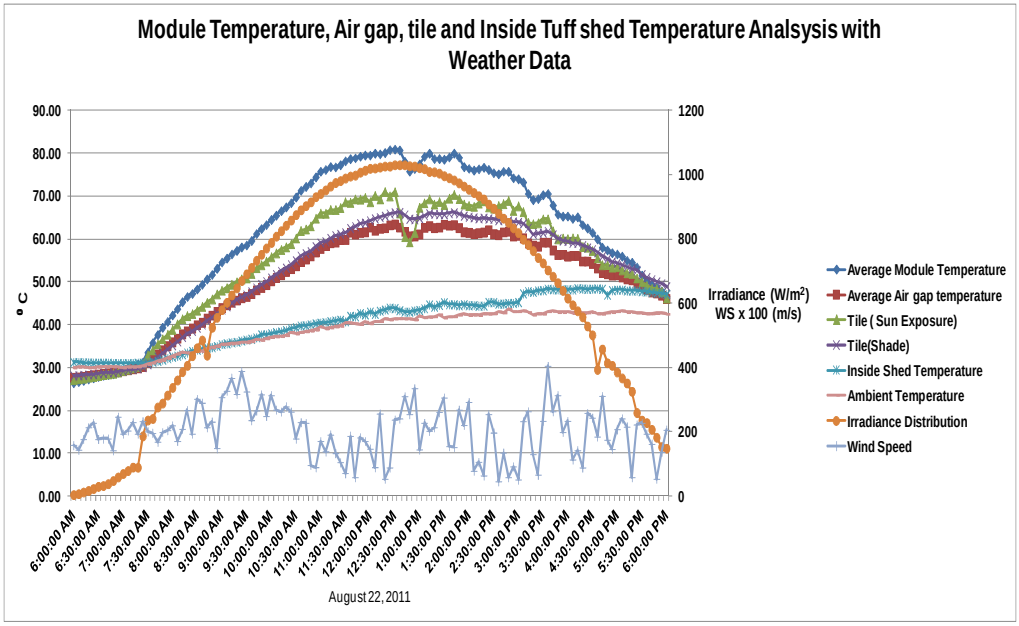

Figure 4.2 Average Array, Air Gap, Inside Shed and Tile Temperature August 22, 2011

In Figure 4.2 it can be noted that the air gap temperature is approximately 20 ºC higher than ambient temperature around mid day conditions. It is also observant that average array temperature is close to 18 º C higher than air gap temperatures during mid day. Air gap is constantly being heated due to heat energy being convected from the module surface into the air underneath the module making it warmer. This in affect results in the rise in module temperature.

If the air gap temperature could be kept lower or close to ambient temperatures, then the large delta in temperature would cause a heat exchange mechanism to develop between module and the air flowing between the air gap, resulting in the modules to become cooler. As it is observant, inside shed temperature constantly increases during the day and does not drop by the end of the day. This is as heat energy radiates through the roof which in essence keeps the inside temperature warm. Also a corresponding effect of Irradiance can be noticed. As the irradiance level increased or decreased, the average array temperature seemed to increase and decrease as well.

4.3 Thermal Models

Several thermal models for temperature prediction are developed in this thesis and are discussed in this section below. Data has been collected during four stages of 14 continuous days each including baseline data collection (Configuration I) period. Thermal models are then separately calculated for each individual module for both the test and control array to understand and predict the effect of ambient conditions on module temperature. Later a model for entire array is predicted for both the control and test array. The method of thermal modeling is based on linear regression, a function which is available in Matlab mathematical software. Matlab based linear regression has been used for the study, where the measured module temperature is taken to be the dependent parameter on three measured independent variables such as Irradiance, wind speed and ambient temperature. The generated coefficients for each Irradiance, ambient temperature, wind speed and Constant values were then used to predict module temperature using the equation shown below

$$Tmod = E * w1 + Tamb* w2 + WS * w3 + C \quad (4.1)$$

Where

Tmod = Module Temperature (˚C)

E = Irradiance (W/m^2)

Tamb = Ambient Temperature (º C)

WS = Wind Speed (m/s)

C = Constant

w1, w2, w3 & C = Derived Coefficients

To ensure an accurate analysis, only data points that are above 50 W/m^2 for irradiance and a wind bin of 0 to 4 m/s are considered. Any high wind speed data above 4 m/s has been eliminated as higher end values would skew the model. Typically higher wind speeds and lower irradiance values are observed towards the early morning and later evening, which are not essential for our study.

Table 4.1 Configuration I Thermal Model for Test Array

Module	Coefficients based on initial 14 day Baseline data (July 2 – July 15)				
Module	Irradiance (w_1)	Tamb (w_2)	WS (w_3)	Constant (C)	R^2 Values
1	0.0338	0.9804	-0.9576	1.3038	0.9209
2	0.0348	1.167	-1.0547	-4.7084	0.9421
3	0.0324	1.0366	-0.9203	-0.4987	0.9305
4	0.033	1.2061	-0.9673	-5.9861	0.9439
5	0.0336	1.0631	-0.9476	-1.3625	0.9364
6	0.0348	1.173	-1.0761	-4.7032	0.9446
7	0.032	1.0838	-1.0049	-1.8203	0.9417
8	0.0334	1.1764	-1.0783	-4.7482	0.9455
9	0.0332	1.0635	-1.0065	-1.1901	0.9389
10	0.0328	1.1689	-1.059	-4.5061	0.9456
11	0.0285	1.1189	-1.0352	-2.7181	0.9435
12	0.0304	1.1314	-1.0817	-3.2534	0.9461
Array	0.0327	1.1141	-1.0158	-2.8493	0.9400

The table above shows coefficients generated for the Configuration I (14 day time period), for the test array. Since this thesis is a study and comparison of a side by side BAPV system, a similar regression analysis was computed for the control array setup adjacent to the test array. The results of the regression are shown in Table 4.2

Table 4.2 Configuration I Thermal Model for Control Array

	Coefficients based on initial 14 day Baseline data (July 2 – July 15)				
Module	Irradiance (w_1)	Tamb(w_2)	WS (w_3)	Constant (C)	R^2 Values
1	0.0324	0.9666	-1.0583	1.8284	0.9120
2	0.0321	1.2606	-1.0573	-7.5118	0.9369
3	0.0321	0.9631	-1.0258	1.884	0.9150
4	0.0343	1.2528	-1.0336	-7.4419	0.9403
5	0.0320	0.9568	-1.0015	2.0828	0.9099
6	0.0342	1.2587	-1.0641	-7.4912	0.9404
7	0.0318	0.9825	-0.9942	1.2541	0.9158
8	0.0350	1.2668	-1.0611	-7.8364	0.9422
9	0.0318	1.0035	-1.0063	0.6326	0.9264
10	0.0332	1.2656	-1.0475	1.2656	0.9364
11	0.0287	1.0655	-1.0169	-1.1837	0.9405
12	0.0305	1.2456	-1.0576	-6.8036	0.9413
Array	0.0323	1.1240	-1.0354	-2.4434	0.9298

To then understand the validity of the model, a quick spot check was performed. Spot check method is necessary to understand both the validity and uniformity for both the array and the model. The results of such spot check for both test and control array are provided in Table 4.3.

Table 4.3 Actual Vs Predicted temperatures using Spot Check Method

	Test Array			Control Array		
Module	Actual Temp (ºC)	Predicted Temp(ºC)	Difference	Actual Temp (ºC)	Predicted Temp(ºC)	Difference
1	67.76	71.17	3.41	66.78	69.67	2.89
2	64.5	72.55	8.05	61.36	69.97	8.61
3	66.04	69.75	3.71	66.57	69.29	2.72
4	62.54	70.65	8.11	63.21	72.18	8.97
5	66.29	71.09	4.80	66.4	69.17	2.77
6	63.35	72.75	9.40	62.7	72.22	9.52
7	63.98	69.57	5.59	65.76	69.00	3.24
8	61.87	71.30	9.43	62.89	73.02	10.13
9	65.76	70.82	5.06	64.88	69.09	4.21
10	61.49	70.63	9.14	61.57	80.12	18.55
11	59.26	66.04	6.78	60.2	65.99	5.79
12	59.56	67.99	8.43	59.08	68.43	9.35
Array	63.53	70.36	6.83	63.45	70.68	7.23

As equation 4.1 for thermal model details, using generated coefficients, employing Matlab based regression analysis and feeding measured ambient data for a particular time of the day, module temperature is predicted and compared against measured module temperature to calculate the difference in the temperature values between measured module temperature and predicted module temperature (calculated value).

The temperature equation for module 1 in Test array as provided below:

Tmodule = E * (0.0338) + Tamb*(0.9804) + WS * (-0.9576) + 1.3038

This regression equation provided an R^2 value of 0.9209

The array temperature equation for the average array temperature:

Tarray = E * (0.0327) + Tamb*(1.1141) + WS * (-1.0158) + (-2.8493)

The coefficients are taken as the average of the derived coefficients.

Similarly, the regression equation for this model provided R^2 value of 0.94.

The temperature equation for module 1 in control array as provided below:

Tmodule = E * (0.0324) + Tamb*(0.9666) + WS * (-1.0583) + 1.8284

The regression equation provided an R^2 value of 0.9120

The array temperature equation for the array average temperature:

Tarray = E * (0.0323) + Tamb*(1.1240) + WS * -1.0354) -2.4434

The regression equation in this case provided the value of 0.9298

The R^2 value for each module and the overall array helped determine how good of a fit the regression equation is.

However a wide range is noted in the predicted value when compared with the actual measured values. This is due to having a large bin of wind speed data which might be causing the variation in the model. To have a better understanding of the use and validity of thermal model, another set of thermal models are developed for 14 day data period when the test array is surrounded by wooden wind blocks from the top, side and bottom and the control array is kept unaltered. The entire combination is named as configuration IV, the last setup. The results of the model are discussed a little later in the chapter below. To better understand the behavior pattern of the array and its mismatch, a quick temperature mismatch calculation is computed for the low wind condition and is provided in Table 4.4 below.

Table 4.4 Mismatch under Low WS condition

Low Wind Speed Date: 7/10/11 Time: 12:00 pm WS : 0.225 m/s WD: 147.6 º			
Test - Control	Mismatch Temperature(ºC)	Test - Control	Mismatch Temperature(ºC)
1	0.98	8	-1.02
2	3.14	9	0.88
3	-0.53	10	-0.08
4	-0.67	11	-0.94
5	-0.11	12	0.48
6	0.65	Array	0.08
7	-1.78		

As it can be observed from the table above, the average of the data is a mere 0.08 indicating a very small mismatch. Majority of the data points are well within the +/- 2 ºC of each other, indicating an identical set of arrays.

To ensure that we have the similar trend in the data set and the arrays still continue to behave in a similar pattern, temperature mismatch is performed for high wind speed data. The results of such computation is provided in Table 4.5

Table 4.5 Mismatch under high WS speed condition

High Wind Speed Date: 7/2/11 Time: 12:00 pm WS : 3.8 m/s WD: 147.2 º			
Test - Control	Mismatch Temperature(ºC)	Test - Control	Mismatch Temperature(ºC)
1	1.31	8	-1.00
2	4.43	9	0.79
3	-2.80	10	-0.19
4	-0.21	11	-0.58
5	0.23	12	0.53
6	0.98	Array	0.39
7	-1.55		

A graph to illustrate the trend of module behavior under low wind speed and high wind speed is plotted and provided in Figures 4.3 and 4.4 below.

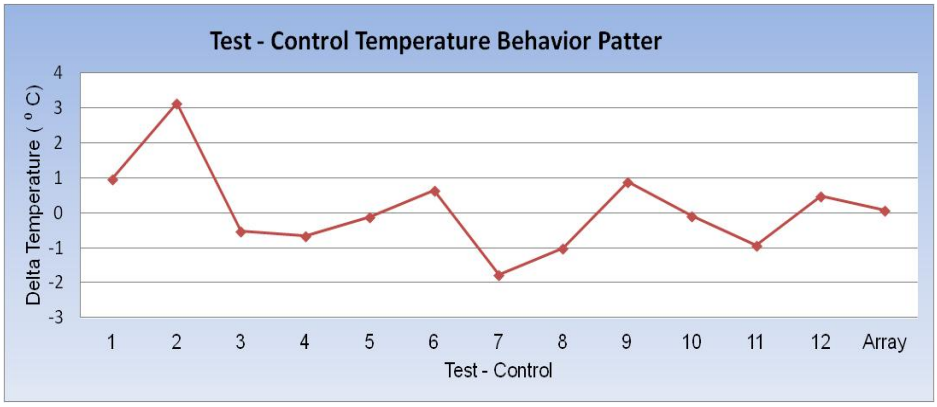

Figure 4.3 Temperature Variance under Low WS (Configuration I)

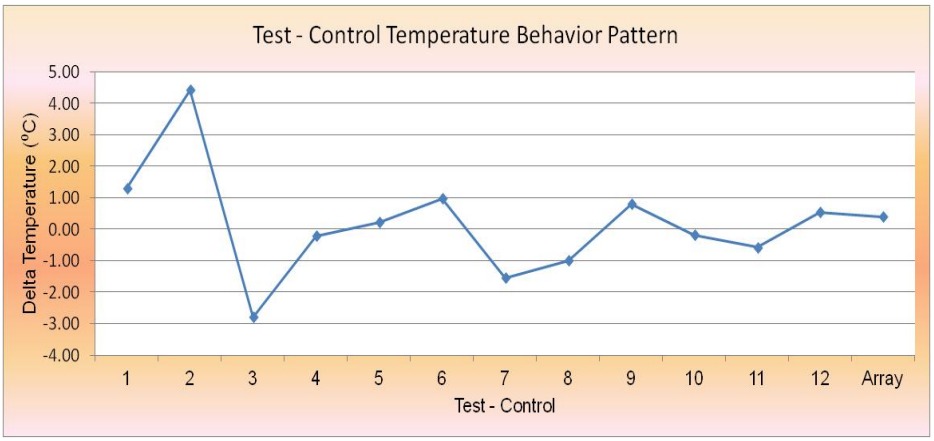

Figure 4.4 Temperature Variance under High WS (Configuration I)

As can be seen from the charts above, Module 1 temperature variance between test and control array is identical (~1ºC) under both low and high wind speed conditions. Similarly module 6 displayed approximately 1 º C temperature variance under low and high wind speed conditions. After observing such bahaviour patterns, it could be inferred that even if module temperatures might go down with high wind speed or rise due to low wind speed, the effect is simultaneous, resulting in very low mismatch between modules placed in similar locations at different arrays making the arrays identical.

4.3.1 Thermal Model for Configuration IV

The table below shows thermal model computed for Test array under high wind speed condition. The coefficients generated are for the data set recorded during the last configuration during which, the test array was sorrounded with wooden blocks on the top, side and bottom. The results of Matlab regression analysis and generated coefficients are provided in Table 4.6

Table 4.6 Generated Coefficients for Test Array (High WS)

	Coefficients based on final 14 day recorded data (August 13–August 26)				
Module	Irradiance (w_1)	Tamb (w_2)	WS (w_3)	Constant (C)	R^2 Values
1	0.0354	1.1987	-0.3849	-6.6289	0.9297
2	0.0362	1.2427	-0.5683	-7.7982	0.9314
3	0.0348	1.2321	-0.4085	-7.357	0.9328
4	0.035	1.288	-0.5611	-9.2352	0.9335
5	0.0356	1.2306	-0.4417	-7.1458	0.9334
6	0.0363	1.2044	-0.5452	-6.2518	0.9343
7	0.0345	1.2416	-0.518	-7.3229	0.9363
8	0.0353	1.2058	-0.5315	-6.1681	0.9359
9	0.0354	1.218	-0.4311	-6.6479	0.9351
10	0.0351	1.2287	-0.6238	-6.7015	0.936
11	0.0366	1.3024	-0.6504	-9.2833	0.9332
12	0.0365	1.2481	-0.8712	-7.2604	0.9328
Array	0.0356	1.2368	-0.5446	-7.3168	0.9337

For comparison purposes, the coefficients for the control array are concurrently provided in Table 4.7 below.

Table 4.7 Generated Coefficients for Control Array (High WS)

	Coefficients based on final 14 day recorded data (August 13–August 26)				
Module	Irradiance (w_1)	Tamb (w_2)	WS (w_3)	Constant (C)	R^2 Values
1	0.0312	0.9568	-0.6141	2.6092	0.8979
2	0.0299	1.4074	-1.2941	-11.7104	0.9305
3	0.0311	0.9506	-0.5838	2.8325	0.9037
4	0.0321	1.3788	-1.1745	-10.9477	0.9322
5	0.0312	0.9363	-0.527	3.2394	0.899
6	0.032	1.3768	-1.2144	-10.758	0.9318
7	0.031	0.9571	-0.5395	2.5367	0.9051
8	0.0327	1.3552	-1.1977	-10.1467	0.933
9	0.0309	0.9815	-0.5954	1.7876	0.915
10	0.031	1.3434	-1.1594	-9.736	0.9333
11	0.028	1.0273	-0.6983	0.4108	0.9297
12	0.0288	1.2802	-1.1164	-7.5242	0.9322
Array	0.0308	1.1626	-0.8929	-3.9506	0.9202

An actual vs predicted temperature analysis is conducted on both for the test and control array to understand the effect of having a more uniform environment in case of test array and also learn if thermal model becomes more consistant when coefficients are more consistant.

Table 4.8 below provides the values for measured and predicted temperatures as discussed above.

Table 4.8 Measured Vs. Predicted Temperature (Configuration IV)

CONFIGURATION IV					
Test Array (All Wind Blocks)			Control Array		
Actual Temp (ºC)	Predicted Temp(ºC)	Difference	Actual Temp (ºC)	Predicted Temp(ºC)	Difference
78.46	78.41	-0.05	69.58	72.34	2.76
80.2	79.19	-1.01	75.1	72.85	-2.25
77.55	78.36	0.81	69.11	72.32	3.21
78.87	78.43	-0.44	76.66	75.15	-1.51
78.22	79.21	0.99	68.82	72.45	3.63
79.32	79.33	0.01	76.48	75.00	-1.48
76.91	78.06	1.15	68.79	72.36	3.57
78.4	78.50	0.10	76.6	75.50	-1.10
78.06	79.02	0.96	69.34	72.31	2.97
78.45	78.36	-0.09	79.22	73.81	-5.41
79.52	80.29	0.77	66.88	69.46	2.58
79.8	79.10	-0.70	70.38	71.28	0.90
78.65	78.86	0.21	71.83	72.90	1.07

To better understand the uniformity and consistancy of the thermal model for this configuration, standard deviation is calculated for generated coefficients such as ambient temperature, Constant and measured vs predicted temperature difference values. The result of such analysis is provided below in Table 4.9

Table 4.9 Coefficients under high WS (Configuration IV)

CONFIGURATION IV					
Test Array (All Wind Blocks)			Control Array		
Ambient Temp	Constant	Difference	Ambient Temp	Constant	Difference
1.1987	-6.6289	-0.05	0.9568	2.6092	2.76
1.2427	-7.7982	-1.01	1.4074	-11.7104	-2.25
1.2321	-7.357	0.81	0.9506	2.8325	3.21
1.288	-9.2352	-0.44	1.3788	-10.9477	-1.51
1.2306	-7.1458	0.99	0.9363	3.2394	3.63
1.2044	-6.2518	0.01	1.3768	-10.758	-1.48
1.2416	-7.3229	1.15	0.9571	2.5367	3.57
1.2058	-6.1681	0.10	1.3552	-10.1467	-1.10
1.218	-6.6479	0.96	0.9815	1.7876	2.97
1.2287	-6.7015	-0.09	1.3434	-9.736	-5.41
1.3024	-9.2833	0.77	1.0273	0.4108	2.58
1.2481	-7.2604	-0.70	1.2802	-7.5242	0.90
1.2368	-7.3168	0.21	1.1626	-3.9506	1.07
SD = 0.03	**SD = 0.98**	**SD = 0.69**	**SD = 0.20**	**SD = 6.29**	**SD = 2.82**

Basically as it is clearly observant from the table above that blocking the array from the top, sides and the bottom is causing the array to be more uniform. The coefficients for ambient temperature for test array display a SD of 0.03 and the coefficient for constant display the standard deviation of 0.98 as compared to 6.29. In other words, even under high wind speed conditions, the system is less turbulent. Evidence of such is seen is when the thermal model predicts the

module temperature within +/- 2 ºC of the actual measured module temperature. This also shows that the thermal model is more consistant and uniform for array with blocks, an added advantage with a cheaper cost of wodden blocks.

The 3D plot below helps depict the turbulent behaviour of ambient temperature and constant coefficients as compared to a more consitant and uniform distribution exhibited from Test array.

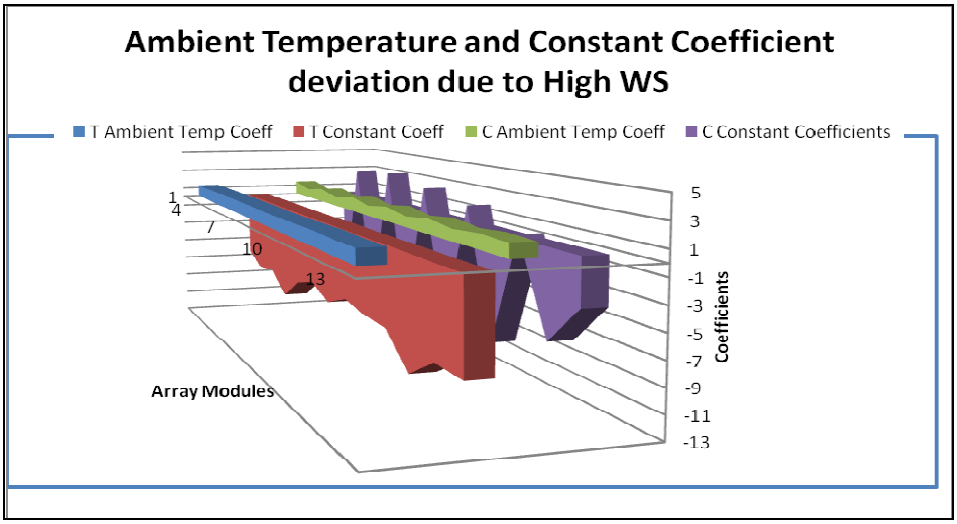

Figure 4.5 3D representation of Generated Coefficients under High WS (Turbulent) conditions

A recent study conducted at ASU-PRL by Jaewon Oh in his thesis [1] discusses on the issues of ambient temperature coefficient and contant coefficient mismatch due to the effect of wind direction variability. He mentioned installing an array more toward the center of the rooftop might help eliminating the turbulance. However it can be noted here that even an array, placed close to the edge of the rooftop under high wind speed conditions can be kept under more controlled conditions if it can be insulated from side and bottom preventing the effect of wind.

As Table 4.9 indicates

- A large deviation from zero in constant coefficients can be noted
- A variation from one in ambient coefficient can be noted, which is more turbulent for control array

As the effect of ambient temperature is more non-uniform through out control array, this would have direct impact on module temperature and its mismatch. Typically as system integrators look to match modules to invertars and eventually look to size array to invertars, it is essential for them to ensure module minimum voltage does not drop below inverter minimum voltage(to ensure MPPT). Ensuring that the average system level temperature is remaining more uniform even under high windspeed conditions, would allow system designers to understand array performance better and match array to inverter better.

4.3.2 Array Tamb Coefficients

4.3.2.1 Configuration I

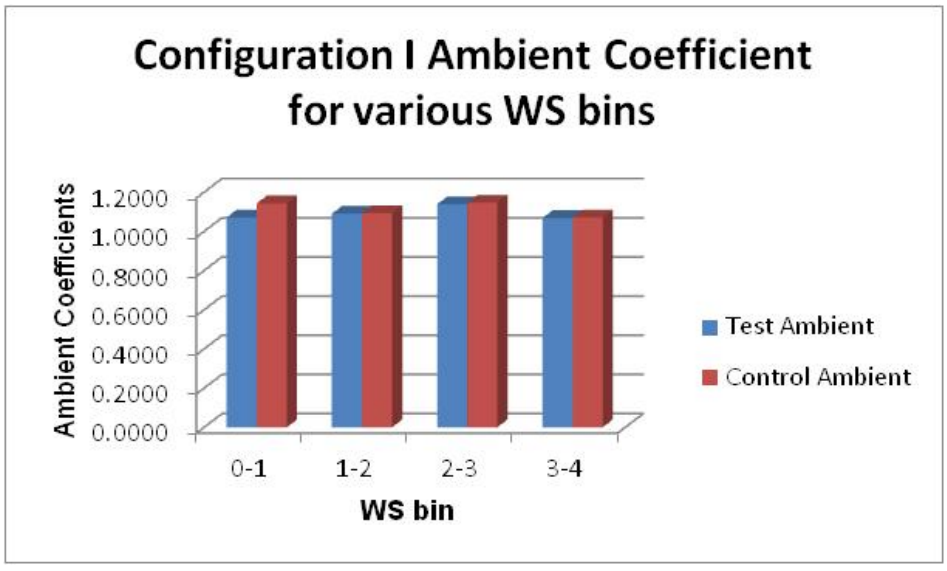

Figure 4.6 Configuration I Coefficient Analysis (Amb T) for Various WS Bins

From the observation above, it can be deduced that

- Both systems are experiencing similar Ambient conditions under varying wind speed conditions
- Both systems are identical with each other and behave identically under different wind speed bins

4.3.2.2 Configuration II

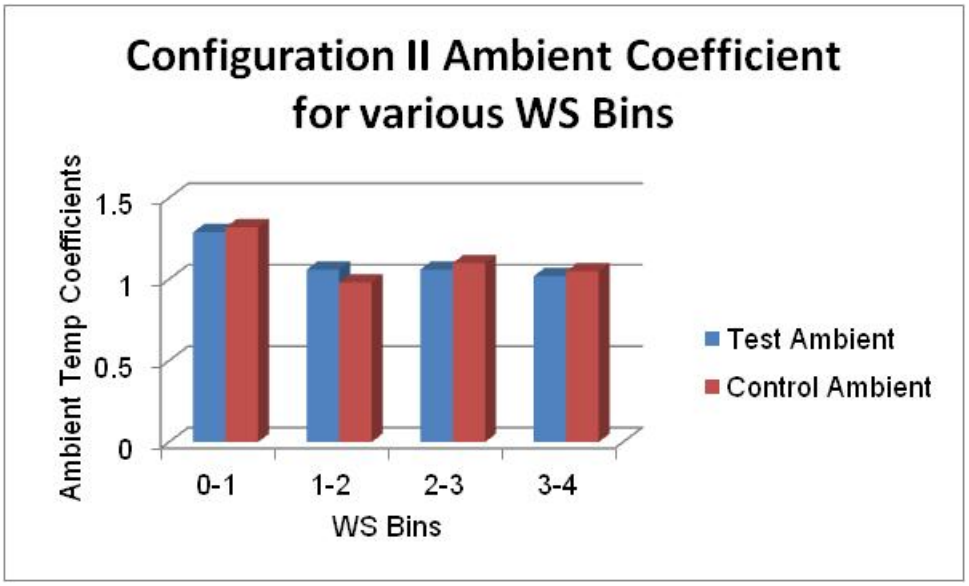

Figure 4.7 Configuration II Coefficient Analysis (Amb T) for Various WS Bins

From the observation above, it can be deduced that

- Fan is having some effect, however there is a slight increase in the ambient temperature coefficients for low WS bin
- The higher ambient conditions, such as higher wind speeds are causing the cooler effect on ambient temperature.
- A possible larger fan under low WS bin might help correct this issue

4.3.2.3 Configuration IV

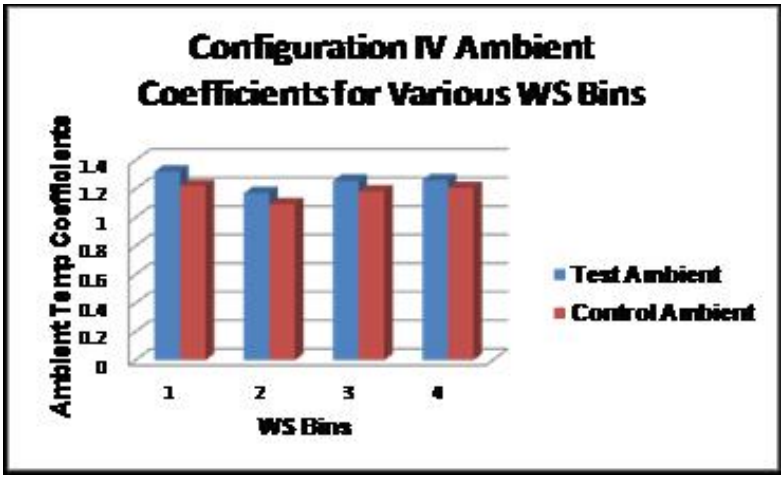

Figure 4.8 Configuration IV Coefficient Analysis (Amb T) for Various WS Bins

It is evident from the graph above that:

- Overall the ambient temperatures are uniform
- The ambient temperature coefficients for Test arrays are slightly higher as compared with the ambient for control. This might be due to the wind blocks blocking any possible air underneath the array, contributing to the ambient temperature effect on the overall module temperature.

4.3.3 Tamb coefficient within 0-1 WS bin for Configuration I, II & IV

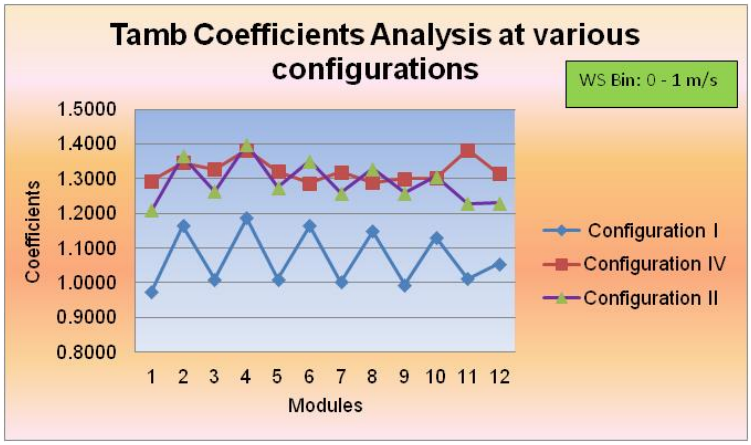

Figure 4.9 Ambient Temperature Coefficients (various Configurations)

The above chart helps display behavior of ambient temperature by means of ambient temperature coefficients, which were calculated using Matlab based regression analysis. The data is presented for each individual module installed in the array, starting from top to bottom, indicated as 1-12. The following observations can be made:

- Coefficients are non-uniform as we progress down the array. There is almost a 0.2 difference in coeffcient value calculated
- For configuration IV and configuration II, the mismatch in ambient temperature effect is mitigated. The overall consistancy in ambient temperature for the entire array is improved which would lead to a more uniform array temperature distribution

4.3.3.1 Irradiance Coefficient within 0-1 WS bin for Configuration I, II & IV

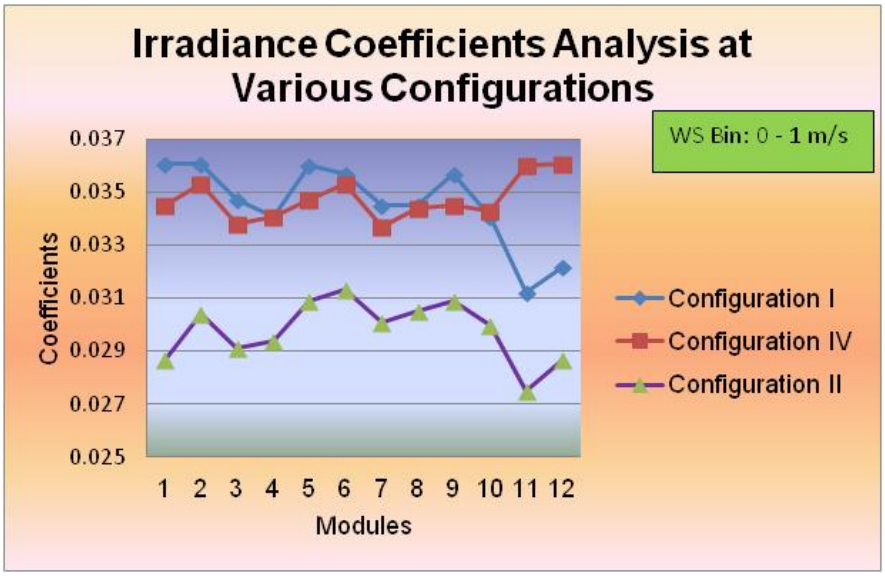

Figure 4.10 Irradiance Coefficients (Various Configurations)

Irradiance coefficients:

- Configuration I and configuration IV display similar irradiance coefficients.

- An interesting drop in coefficients is seen when fan is implemented (Configuration II) and turned on. The coefficients follow similar trend.
- However, the instant wind blocks are place, the drop is eliminated and coefficients are set back to the original pattern observed in the configuration I data set.
- It is evident that the wind blocks are causing an elevation in system temperature, causing the shift in temperature. For future studies, this graph can be an essential tool to benchmark different capacity fans to see their effectiveness in cooling the system.

4.3.4 Temperature Uniformity

Temperature uniformity is a major concern for utility and system integrators. It is especially important when it comes to grid stability, system design, and sizing modules to inverters for optimum yield. Inverters manufacturers need to ensure that inverters are operating within the specified MPPT range and do not fall out of the minimum voltage range specified. This section elaborates on temperature mismatch issues experienced by a typical residential system and how it can be mitigated under low and high wind speed conditions. Four configurations (Configuration I, Configuration II, Configuration III & Configuration IV) are analyzed and discussed in the sections below.

4.3.4.1 Configuration I (Low WS)

Both wind speed and direction tend to have an impact on module temperature and array temperature uniformity. In a recent study conducted by another graduate student, Jonathan Hrica[3] at Arizona State University it was published that the array tends to be slightly more uniform during low wind speed conditions and display more non uniformity during high wind speed conditions. This thesis

helps further explore the analysis by comparing two side by side BAPV systems comparing them under similar ambient conditions such as both under low and high wind speed conditions. Both side by side systems are executed through a set of configuration installs, which are detailed in the abstract section of the thesis. The results of the analysis are provided below.

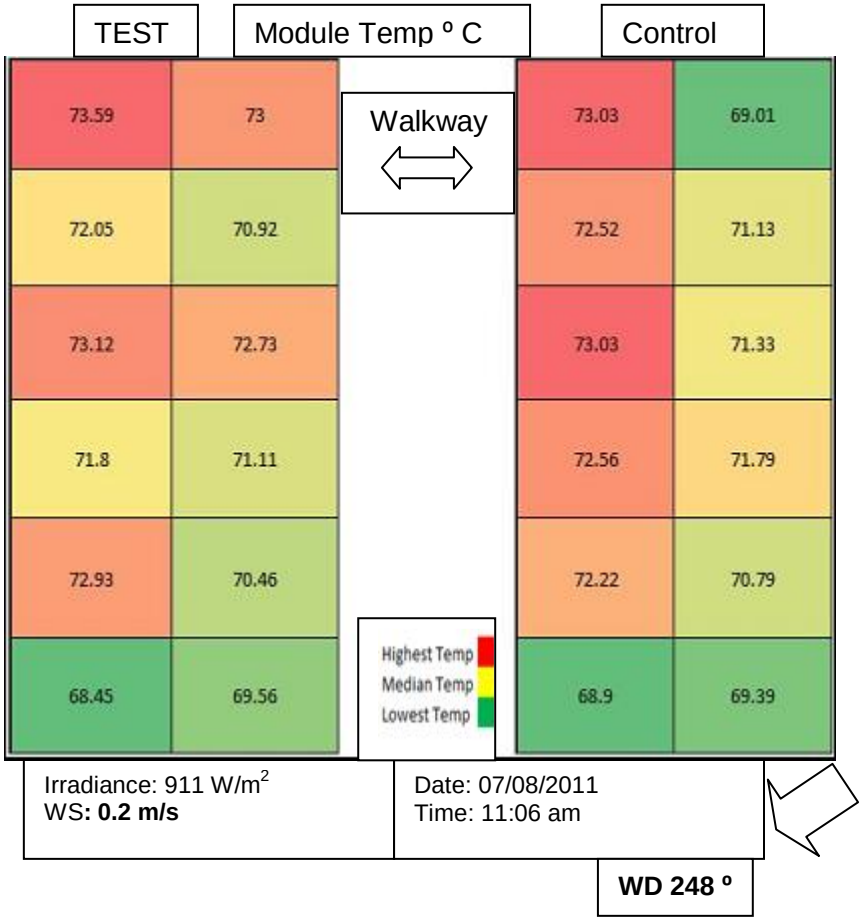

Figure 4.11 Effect of Low WS for Configuration I

The above figure shows module temperature recorded under for both arrays under low wind speed conditions. A mismatch table (temperature distribution) has been calculated for both arrays and is shown below.

Table 4.10 Configuration I Thermal Mismatch (Low WS)

Modules	Test	Control
1	73.59	73.03
2	73.00	69.10
3	72.05	72.52
4	70.92	71.13
5	73.12	73.03
6	72.73	71.33
7	71.80	72.56
8	71.11	71.79
9	72.93	72.22
10	70.46	70.79
11	68.46	68.90
12	69.46	69.39
Max ºC	73.59	73.03
Min ºC	68.46	68.9
Delta ºC	5.13	4.13
Side By Side Delta = 1		

4.3.4.2 Configuration I (High WS)

To understand if high wind speed causes any interesting behavior and throws the array into a highly non uniform behavior, a similar approach was undertaken to the analysis conducted for low wind speed conditions. The results of such are provided below.

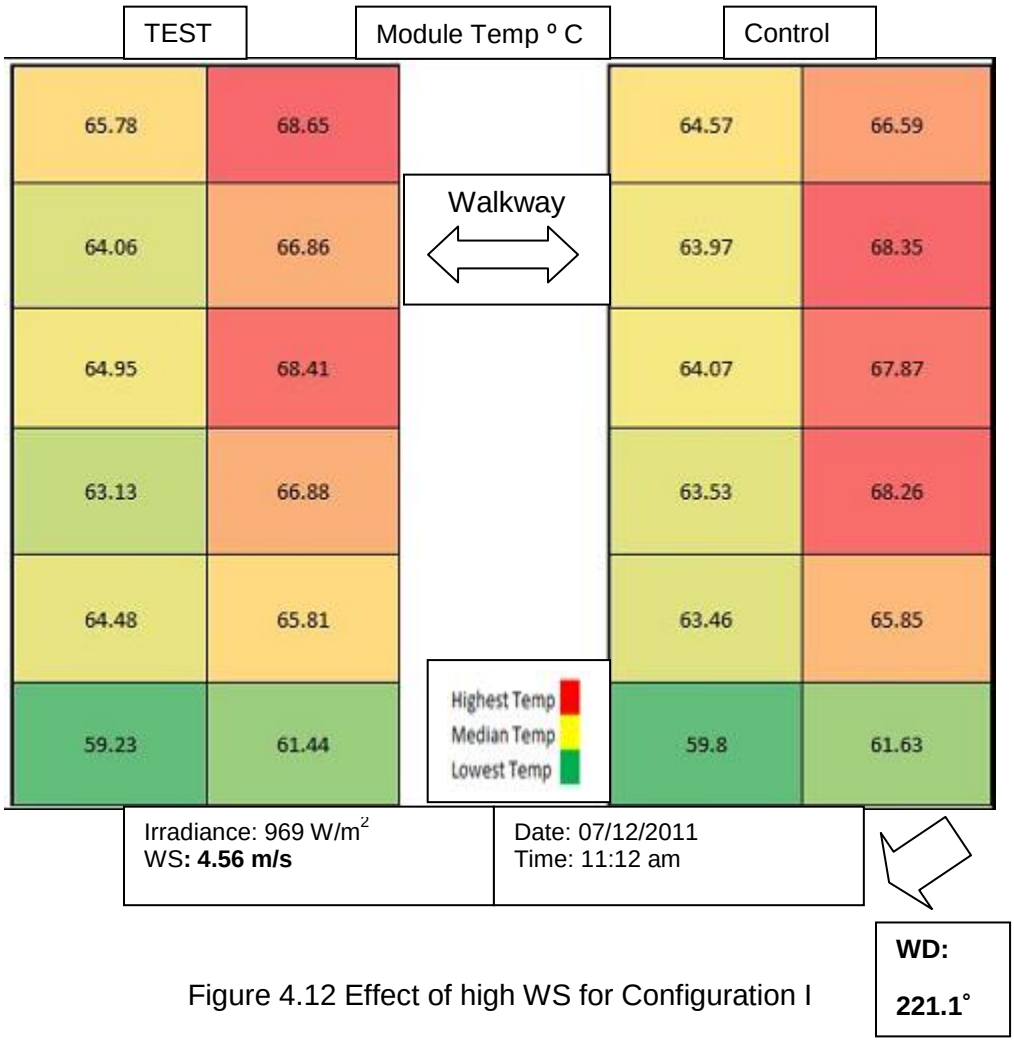

Figure 4.12 Effect of high WS for Configuration I

A table on the next page is provided to help understand the temperature mismatch for the baseline configuration under high wind speed conditions.

Table 4.11 Configuration I Thermal Mismatch (High WS)

Modules	Test	Control
1	65.78	64.57
2	68.65	66.59
3	64.06	63.97
4	66.86	68.35
5	64.95	64.07
6	68.41	67.87
7	63.13	63.53
8	66.88	68.26
9	64.48	63.46
10	65.81	65.85
11	59.23	59.82
12	61.44	61.63
Max ºC	68.65	68.35
Min ºC	59.23	59.8
Delta ºC	9.42	8.55
Side By Side Delta = 0.87 º C		

The following identifications can be made

- Temperature Mismatch is noticed in Test & Control arrays.
- Latent heat movement to the top from bottom of the array also known as the chimney effect is noticed.
- **Both arrays seem to be identical under high and low WS conditions as the side by side delta calculated between them remains to be within less than +/- 1ºC.**

4.3.4.3 Configuration II (Low WS)

Soon after looking at configuration I, Configuration II of the thesis looked into having a fan installed into the test array and its effect of array temperature uniformity, both under low and high wind speed conditions. An image of the setup is provided below

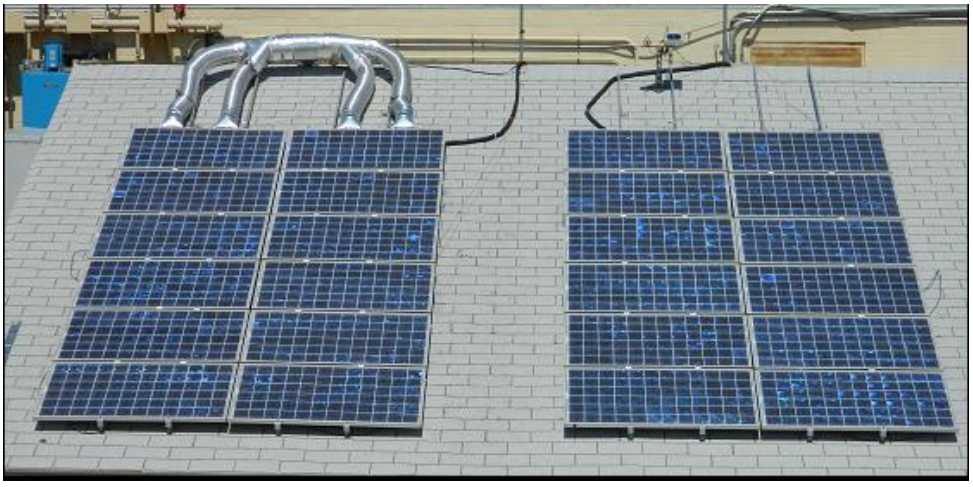

Figure 4.13 Configuration II Conceptualization and Setup

The drawing next page details the layout and results obtained for configuration II of the thesis.

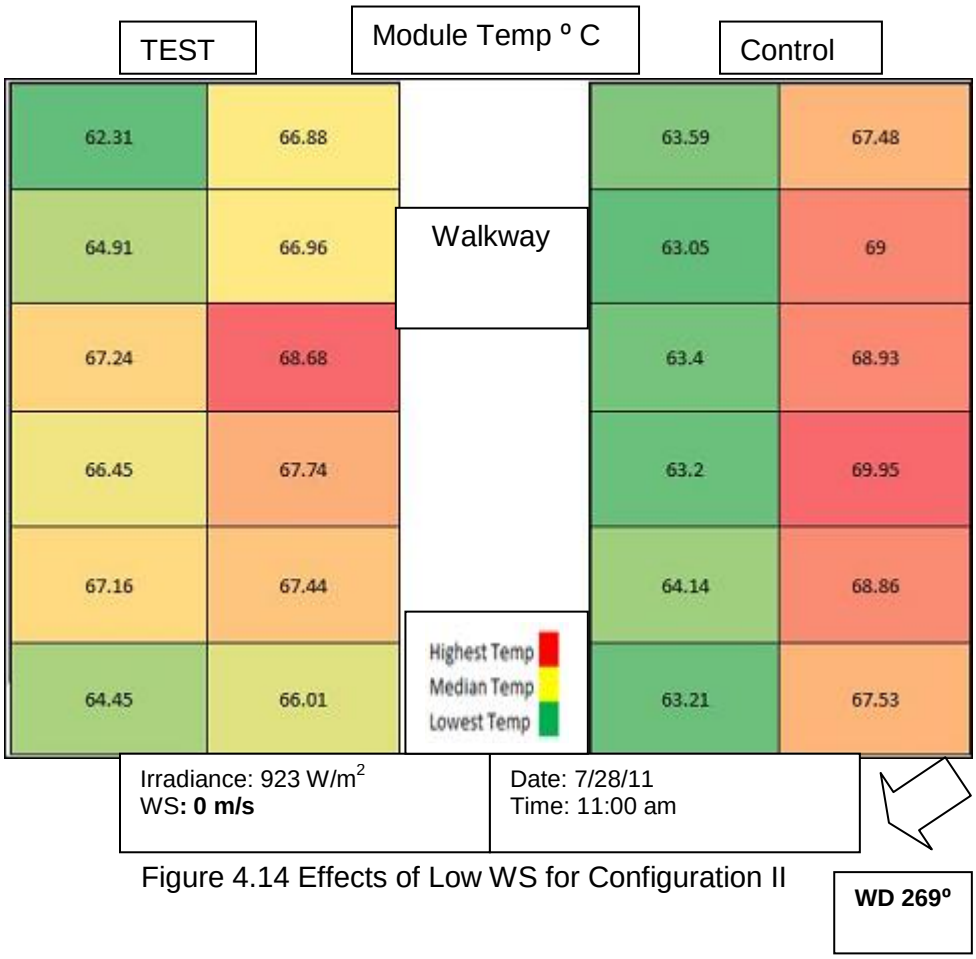

Figure 4.14 Effects of Low WS for Configuration II

Theoretically the fan should help exhaust the hot stagnant air which is building underneath the array and in effect help cool the array. As a result, we should be expecting a smaller delta temperature for the array under the effect of fan as compared to the array similar to baseline conditions. The results of such findings are provided in table below

Table 4.12 Configuration II Thermal Mismatch (Low WS)

Modules	Test	Control
1	62.31	63.59
2	66.88	67.48
3	64.91	63.05
4	66.96	69.00
5	67.24	63.40
6	68.68	68.93
7	66.45	63.20
8	67.74	69.95
9	67.16	64.14
10	67.44	68.86
11	64.45	63.21
12	66.01	67.53
Max ºC	**68.68**	**69.95**
Min ºC	**62.31**	**63.05**
Delta ºC	**6.37**	**6.9**
Side By Side Delta = -0.53 ºC		

4.3.4.4 Configuration II (High WS)

Similarly, the fan effect on array temperature uniformity under high wind speed was looked into as well. The results of such finding are presented below.

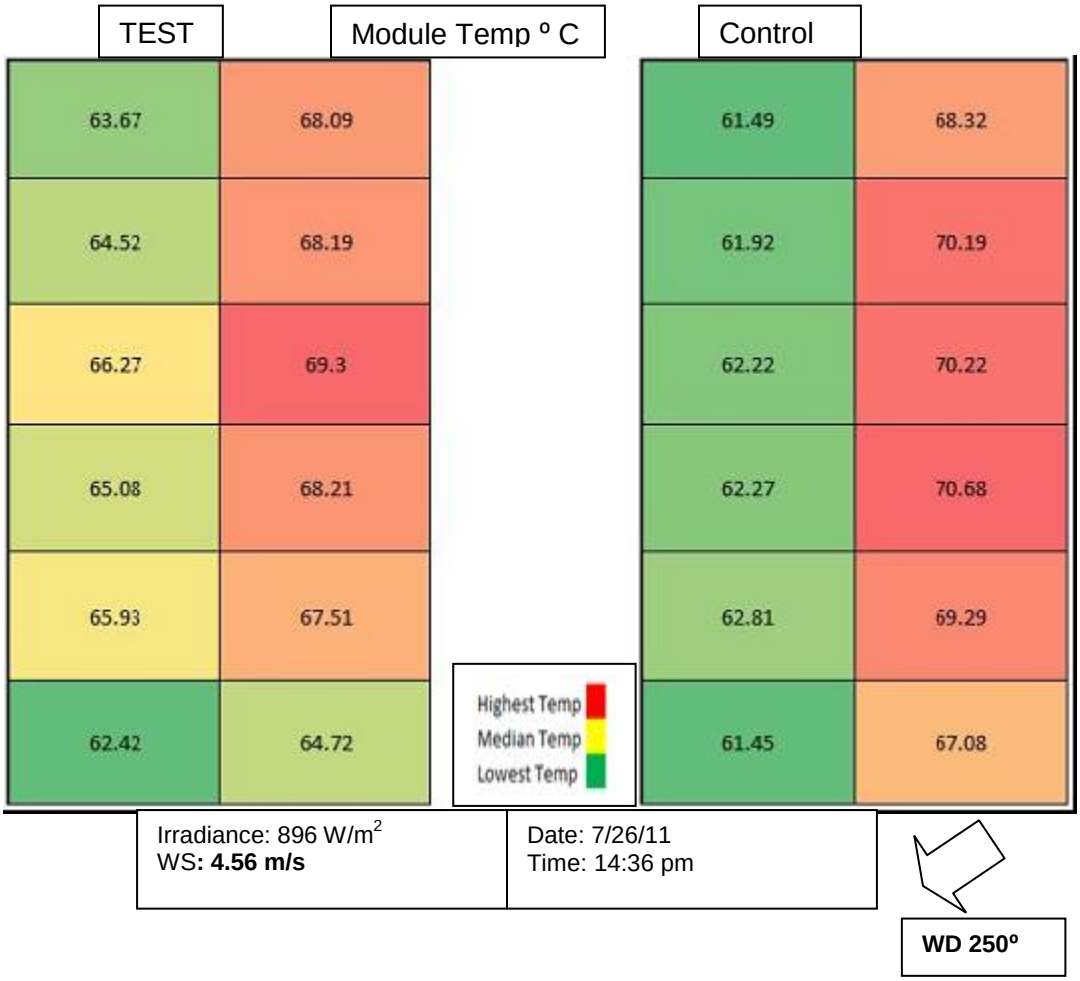

Figure 4.15 Effects of High WS on Configuration II

Table 4.13 Configuration II Thermal Mismatch (High WS)

Modules	Test	Control
1	63.67	61.49
2	68.09	68.32
3	64.52	61.92
4	68.19	70.19
5	66.27	62.22
6	69.3	70.22
7	65.08	62.27
8	68.21	70.68
9	65.93	62.81
10	67.51	69.29
11	62.42	61.45
12	64.72	67.08
Max ºC	**69.3**	**70.68**
Min ºC	**62.42**	**61.45**
Delta ºC	**6.88**	**9.23**
Side By Side Delta = -2.35 ºC		

The following identifications can be made

- It is evident that few modules on top row (test) are cooled due to fan having a cooling effect, both under low and high wind speed conditions
- Test system continues to remain uniform even under high wind speed conditions. Side by side delta increases to -2.35 ºC under high wind speed conditions, a sheer indications that the control system is experiencing higher mismatch

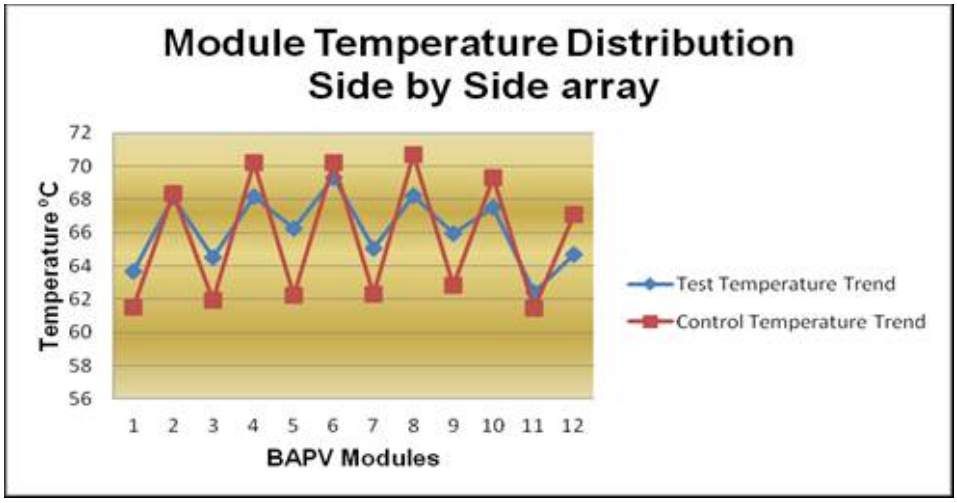

Figure 4.16 Module Thermal Uniformity (Configuration II)

As can be seen from the temperature distribution chart in Figure 4.12, a typical variance in intermodule temperatures can be seen ranging from 6ºC to 8ºC in the control array. The Test array is slightly more uniform where the inter module temperature shifts are ranging from +/- 4ºC.

4.3.4.5 Configration III (LWS)

Fig 4.17 Configuration III Conceptualization and Setup

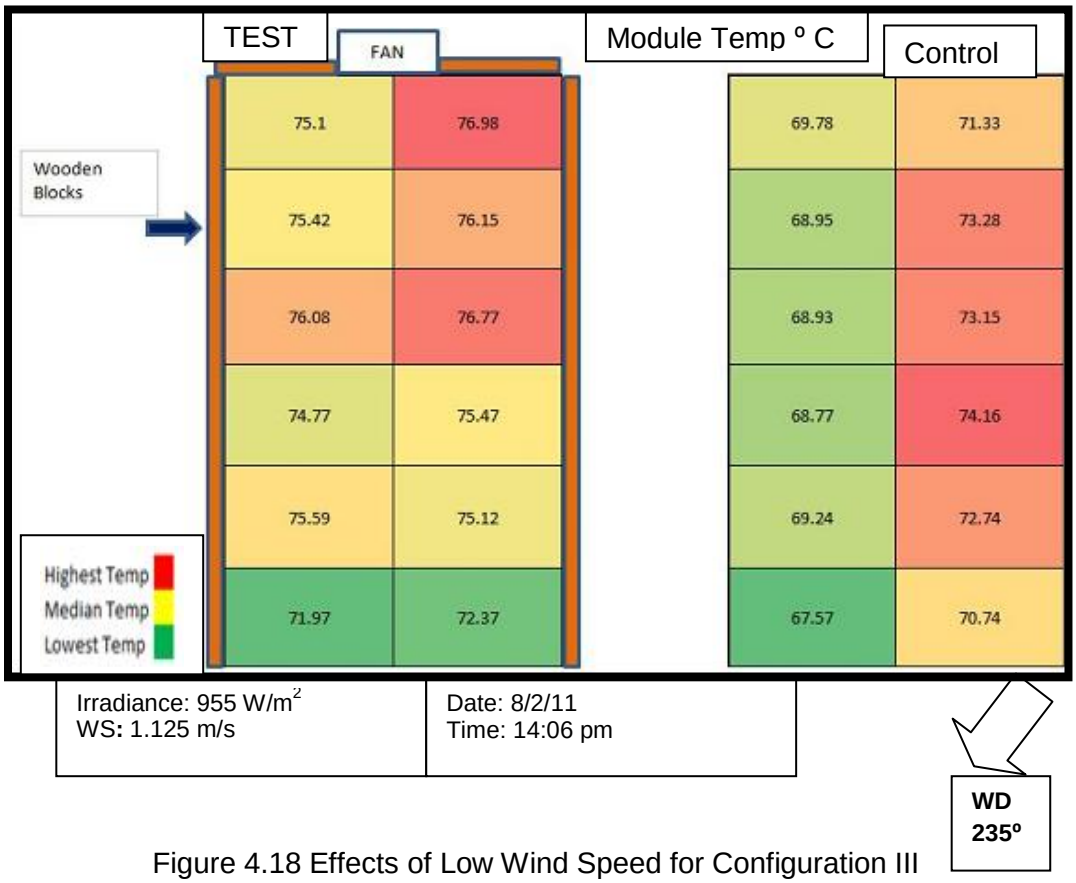

Figure 4.18 Effects of Low Wind Speed for Configuration III

Similarly for comparison and analysis purposes a table is provided below, to understand the mismatch and uniformity for individual arrays.

Table 4.14 Configuration III Thermal Mismatch (Low WS)

Modules	Test (ºC)	Control (ºC)
1	75.1	69.78
2	76.98	71.33
3	75.42	68.95
4	76.15	73.28
5	76.08	68.93
6	76.77	73.15
7	74.77	68.77
8	75.47	74.16
9	75.59	69.24
10	75.12	72.74
11	71.97	67.57
12	72.37	70.74
SD	**1.54**	**2.17**
Max ºC	**76.98**	**74.16**
Min ºC	**71.97**	**67.57**
Delta ºC	**5.01**	**6.59**
Side By Side Delta = -1.58 ºC		

4.3.4.6 Configuration III (High WS)

The results obtained for side wind blocks under high wind speed conditions are provided below. Both the temperature behavior patter and side by side analysis tabulated data is provided below

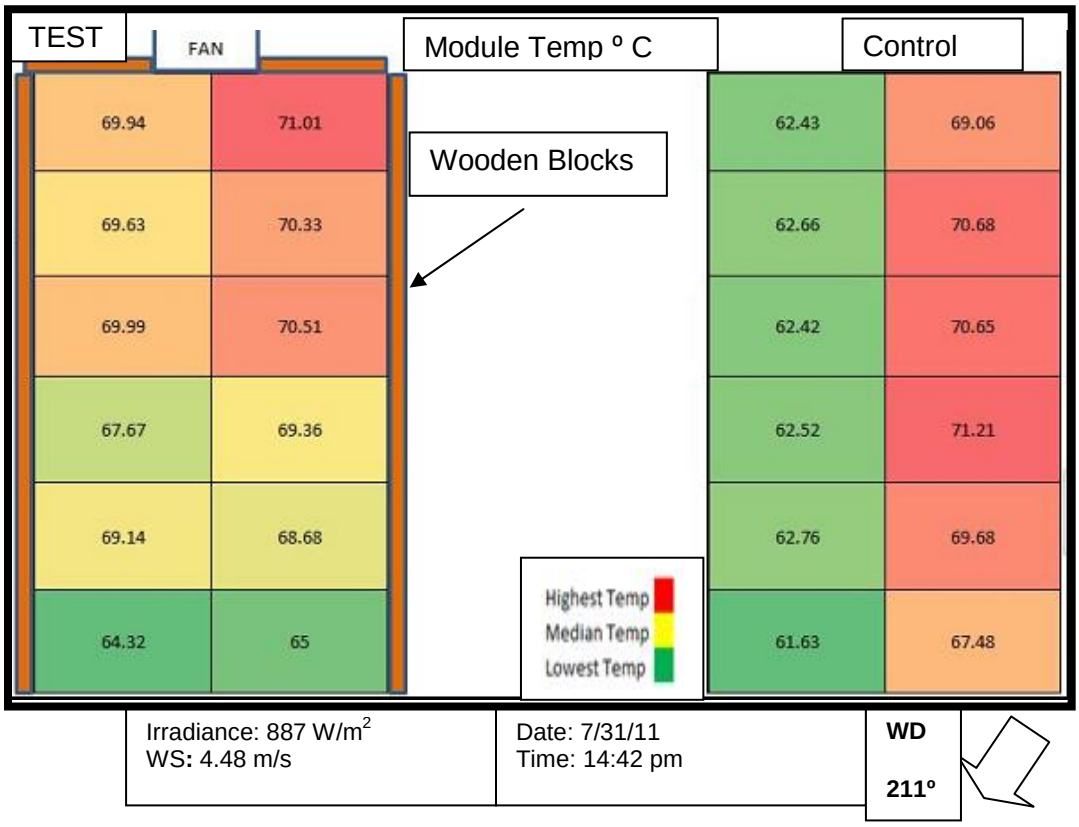

Figure 4.19 Effects of High Wind Speed for Configuration III

Table 4.15 Configuration III Thermal Mismatch (High WS)

Modules	Test (ºC)	Control (ºC)
1	69.94	62.43
2	71.01	69.06
3	69.63	62.66
4	70.33	70.68
5	69.99	62.42
6	70.51	70.65
7	67.67	62.52
8	69.36	71.21
9	69.14	62.76
10	68.68	69.68
11	64.32	61.63
12	65	67.48
SD	**2.13**	**3.98**
Max ºC	**71.01**	**71.21**
Min ºC	**64.32**	**61.63**
Delta ºC	**6.69**	**9.58**
Side By Side Delta = -2.89 º C		

The following identifications can be made

- It is evident that the inter-row module temperatures are not varying significantly for the test array as there is hardly any parasitic airflow from the sides and top.
- For example, temperature difference between module 1 & 2 in test array is ~1ºC (71.01-69.94)

- Temperature difference between module 1 & 2 in control arrays is ~7ºC (69.06 - 62.43)
- Similarly overall Test array standard deviation is 2.13 ºC whereas; control array Standard deviation is slightly higher at 3.98 ºC, making it more non-uniform.

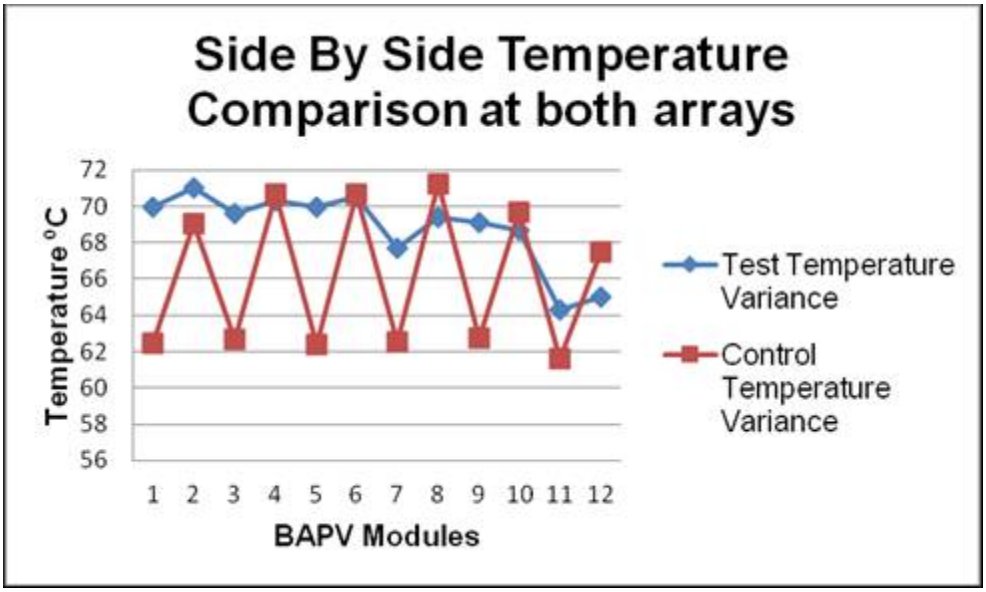

Figure 4.20 Module Thermal Uniformity (Configuration III)

As it is clearly seen from the chart above, placing wind blocks sorrounding the array enhances the thermal stability which was initially discussed in Figure 4.12 which showed the effect of just having the fan in place. Although the overall array temperature increases slightly, it is compensated due to a mitigation in temperature mismatch.

4.3.4.7 Configuration IV (High WS)

The last and final configuration (Configuration IV) of this analysis deals with completely insulating the test array with wind blocks. The goal here is to see if thermal mismatch is mitigated even further for the test array when it is completely sorrounded from wooden blocks. Hence the results are provided for the worst case (High Wind Speed) data below.

For the analysis, the wind blocks have been placed on the top, side and bottom of the array with fan on condition (continuos). An image of the setup is provided below for clarity.

Figure 4.21 Configuration IV Conceptualization & Setup

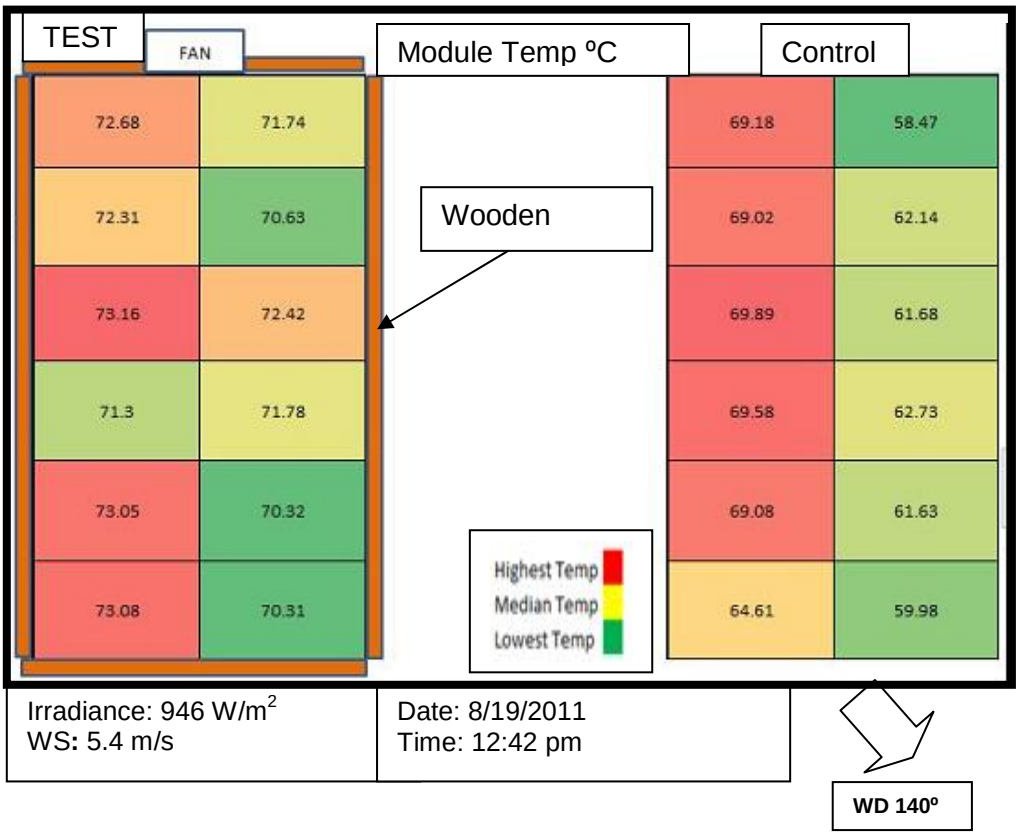

Figure 4.22 Effect of High Wind Speed for Configuration IV

Table 4.16 Configuration IV Thermal Mismatch (High WS)

Modules	Test (ºC)	Control (ºC)
1	72.68	69.18
2	71.74	58.47
3	72.31	69.02
4	70.63	62.14
5	73.16	69.89
6	72.42	61.68
7	71.3	69.58
8	71.78	62.73
9	73.05	69.08
10	70.32	61.63
11	73.08	64.61
12	70.31	59.98
SD	**1.06**	**4.25**
Max ºC	**73.16**	**69.89**
Min ºC	**70.31**	**58.47**
Delta ºC	**2.85**	**11.42**
Side By Side Delta = -8.57 ºC		

The following identifications can be made

- As predicted, including wind blocks for the test array from the top, side and bottom is evident in mitigating the thermal mismatch experienced from test array.
- Standard deviation for temperature data for all 12 modules in the array is 1.06 ºC, a value very close to 1 indicating a good fit data and extremely

low variation. However, standard deviation calculated for control array under high wind speed resulted in 4.25 ºC, clearly indicating a large variation in data set

- Standard deviation is backed by the large delta calculated for control array(11.42 ºC) as compared to a small delta for test array (2.85 ºC)

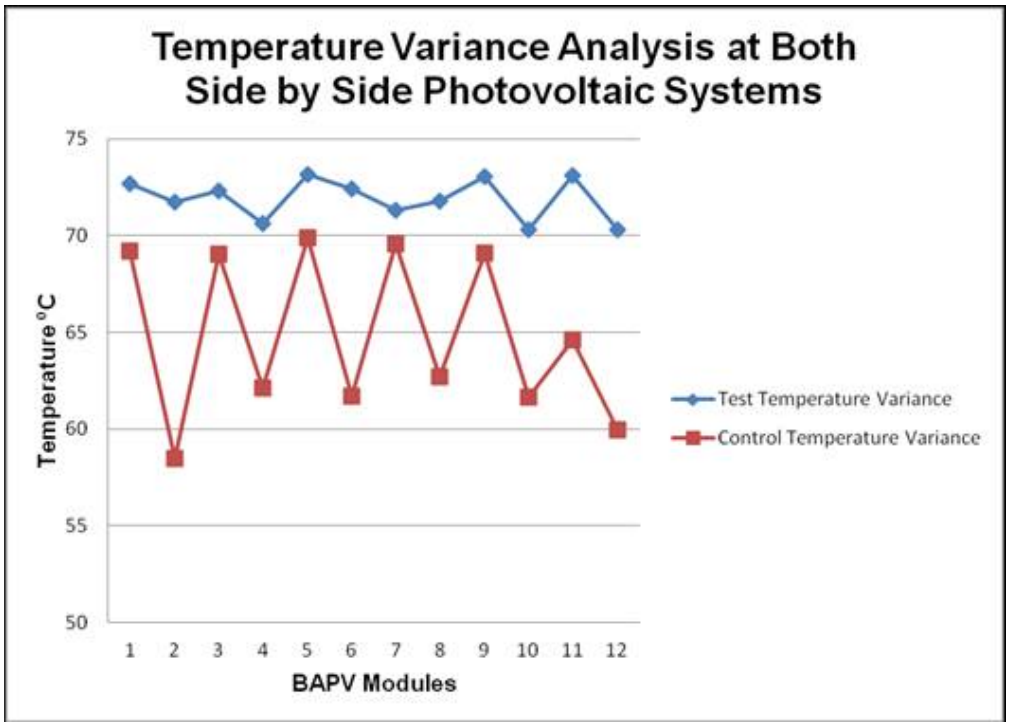

Figure 4.23 Configuration IV and Module Thermal Uniformity

- Insulated array is operating at slightly more higher temperature compared to control array
- This could be due the 40 Watt fan, not being sufficient enough in exhausting the entire hot air which is accumulating under the BAPV system. The hot stagnant air now is in fact a contributor in raising the system temperature.

- The sudden temperature drop experienced by the modules in the lowest row (module 11 & 12) is now eliminated by having a wooden block at the bottom.
- However, the overall system is more thermally uniform, has lower temperature swings and would result in more accurate voltage and power output as compared to the control system with a higher more varying mismatch.
- Although having wooden blocks surrounding the system is causing the overall system temperature to elevate at this point (due to ineffective fan) but the effect is compensated by having a more accurate system.

4.3.5 Fan Effect: Array Row Level I-V measurement and Performance

4.3.5.1 Configuration I row level I-V measurement

For this part of the thesis, several experiments were conducted where multiple I-V measurements were taken at row level to understand the effect of temperature towards the top of the array as compared to the bottom. I-V curves of the entire array were also taken and are compared in the later section.

As discussed in the temperature uniformity section above, a typical BAPV array constantly undergoes a chimney effect, where hot air travels towards the top of the array, keeping the modules towards the top relatively hotter compared to the bottom. A higher temperature would affect module Voc due to the negative temperature coefficient characteristics which would lead to a lower power output.

Both the test and control array were separated in rows of 6 each, where modules were connected in two's to ensure a lower potential and enforce safety. I-V curves were then measured using a Daystar Photovoltaic Curve Tracer, using IVPC 2.63 software platform. The figure below helps show the connection to the curve tracer with the array:

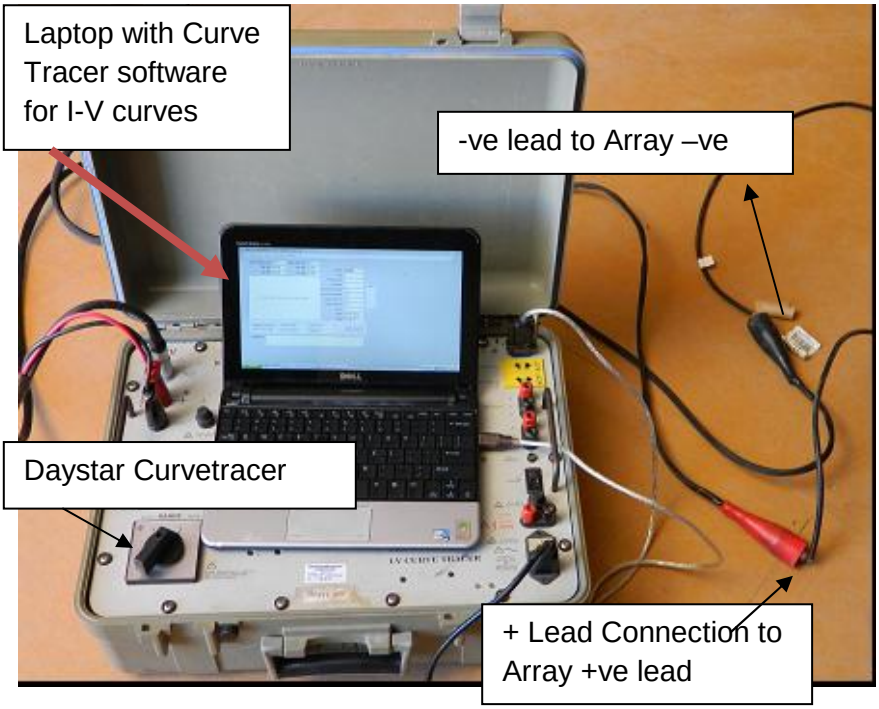

Figure 4.24 Daystar IV curve tracer

Irradiance data and module temperature data were obtained from CR 1000 Campbell scientific data acquisition system. As the I-V curve measurements were inter-row, the Voc and Pmax values varied due to variation in irradiation and temperature. A variation in irradiance effected measured Pmax values and the temperature mismatch between rows affected open circuit voltage.

As a result, both Pmax and Voc values were corrected for irradiance and temperature using the equations below and the graphs are provided in the appendix for convenience. The STC correction equation was

developed based on the fact that c-Si modules typically experience a negative temperature coefficient of power rated at -0.5% for every degree rise in temperature. Also, since the measurements were not recorded at perfect sun (1000 W/m^2), a factor for irradiance correction has been incorporated in the equation.

Pmax Correction:

$$Pmsd * [(1000/E) + (0.5\%*(Pmax*(Tcell-Tref)))] \quad (4.2)$$

Where:

Pmsd = Measured Power (W)

E = Measured Irradiance (W/m^2)

Pmax = Nameplate Rating (W)

Tcell = Measured Temperature

Tref = STC temperature (25ºC)

For our case the nameplate rating value used is (95 x 2 = 190 W) since the I-V curve taken at one time is for two modules connected in series. Similarly the measured temperature is the average of the two measured module temperatures.

Measured Open Circuit Voltage correction [14]:

$$Vtrans = Vref + [Tcell – Tref] \times Cv \quad (4.3)$$

Where:

Vtrans = Measured Open Circuit Voltage

Vref = Voltage at STC condition

Tcell = Measured Cell Temperature

Tref = STC temperature (25 ºC)

Cv = Temperature Coefficient in V/ºC

The temperature coefficient value considered is -0.4%/ºC/module. Hence for two modules connected in series, the temperature coefficient considered is -0.3456V/ºC as the nameplate Voc rating for Photowatt modules is 43.2 Voc/module.

However it was interesting to see the behavior of measured Pmax and Voc and their characteristics with temperature and irradiance. The STC converted chart can be referred to in Appendix A of the thesis.

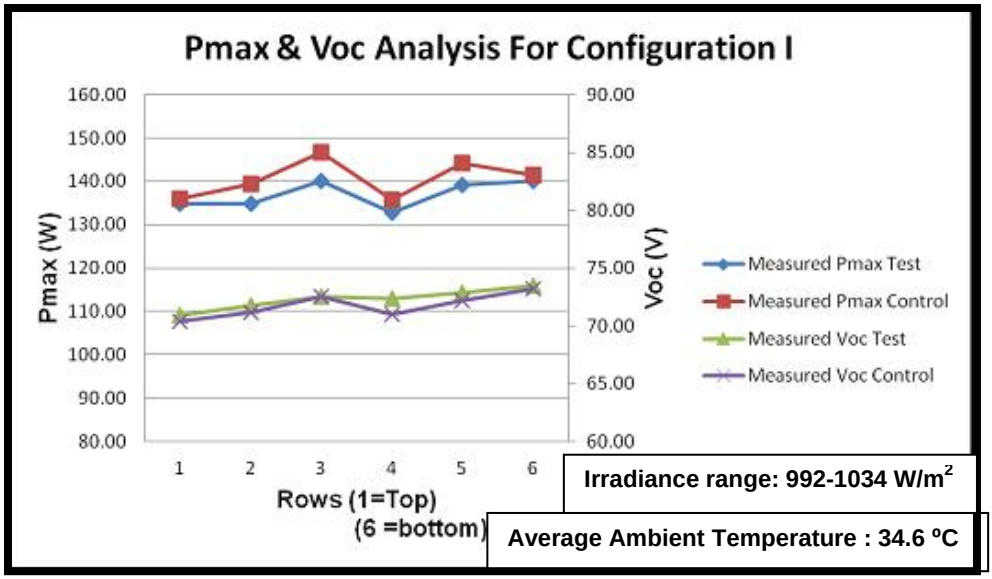

Figure 4.25 Pmax & Voc Analysis (Configuration I)

It is evident from the figure above that

- As we move down the array, open circuit voltage is effected due to higher temperatures developing towards the top part of the array compared to the bottom. This is an attribute due to chimney effect.
- Open circuit voltage and Pmax (Peak Power) seem to be directly proportional. As can be noted as there is an increase in open circuit voltage, it correlates to an increase in peak power as well.

- The gap between measured power and STC power is due to the issues such as temperature, proximity to rooftop, irradiance and soiling. Multiple factors would lead to less power output than expected.

4.3.5.2 Configuration II

Power mismatch is a major issue in the industry today. As mentioned earlier in the discussion, temperature mismatch is a major contributor to voltage irregularity, which eventually leads to power mismatch. A quick experiment was conducted on the test array under fan on conditions to see if running the fan and performing I-V has any improvement on system performance and mismatch compared to the mismatch experienced to a system under baseline conditions. Again, the Pmax values are normalized for STC conditions to eliminate any irradiance and temperature irregularities and the chart can be referrenced in Appendix A.

The trend for the measured data are presented below:

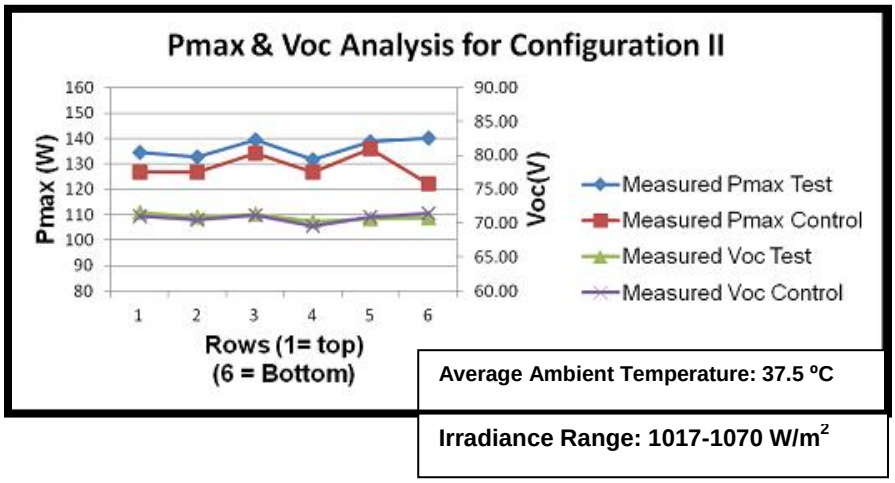

Figure 4.26 Pmax & Voc Analysis (Configuration II)

It is evident from the figure above that:

- Fan certainly helps is reducing the thermal mismatch pattern experienced by the array.
- Overall system power is more consistent. The sharp spike experienced by the panels, or in other words, the mismatch experienced by panels in row 3 is significantly lower compared to the array under no fan operation.
- There is a sudden drop in Pmax value observed in control system towards the bottom of the array, whereas the test is more uniform throughout.

4.3.5.3 Configuration IV

I-V curves of the test array sorrounded by wind blocks and under Fan operation were taken to see if blocking parasitic air flow from the sides would help enhance the performance of the fan even further, which in turn would help cool the array and improve performance. The results of the I-V analysis are provided below for better clarity. The STC chart may be referenced under Appendix A.

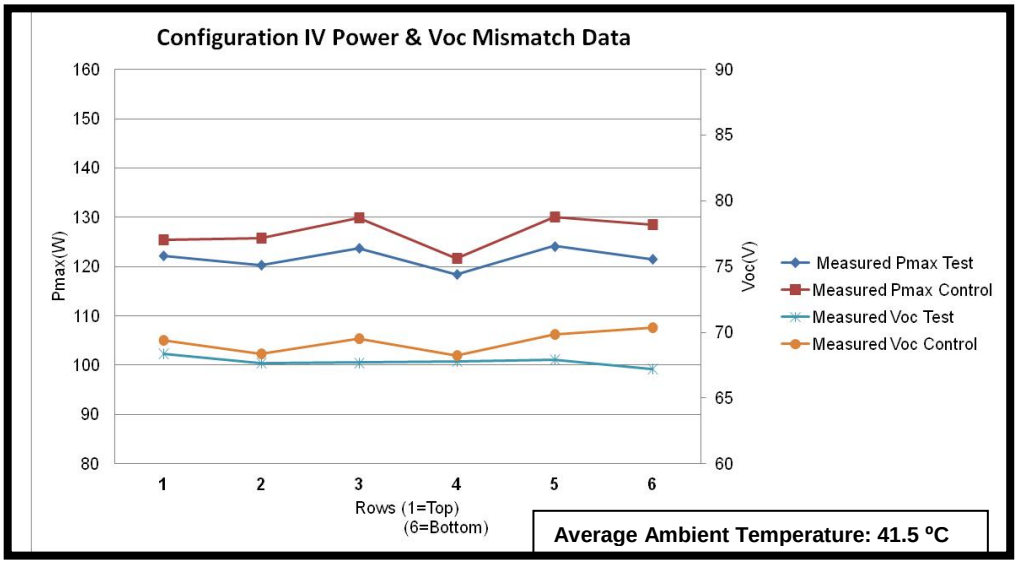

Figure 4.27 Pmax & Voc Analysis for Configuration IV

The following observations are critical in the graph above:

- Surrounding the test array with wooden wind blocks led to a drop in overall system power as the blocks prevented any possible ventilation
- The fan did not prove to be effective in this scenario in pulling the hot stagnant air underneath the system.
- The high temperature also led to a lower overall system Voc for test array
- However, the Voc (open circuit voltage) is more uniform and consistent as compared with control array
- The control array experiences a sharp spike for the bottom string, possibly due little cooler temperatures.

4.3.5.4 Row level I-V sum (STC) Vs Array Level I-V sum (STC)

The modules in both the test and control array were individually connected in series to obtain a single string of 12 modules each. I-V curves of the system were then obtained through configuration I, II and IV. The I-V curves of the entire array IV, converted to STC were then compared with row level I-V curves in STC format. The results of the analysis are presented below:

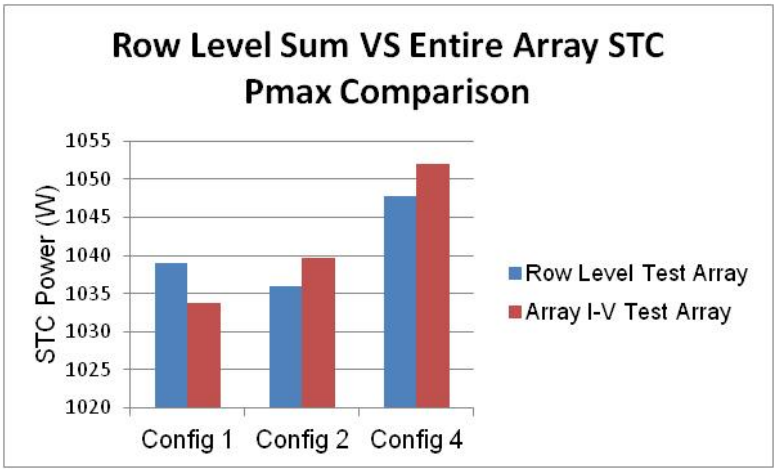

Figure 4.28 STC Pmax analysis for Row level sum Vs Entire Array

A quick percentage difference analysis was conducted on the above figure and is presented below. The equation used for the percentage difference is as follows:

[(Entire Row sum – Array sum)/ Entire row sum] (4.4)

The results of the analysis are as follows:

Table 4.17 Percentage Difference Calculation

Configuration	% difference
I	0.50
II	-0.37
IV	-0.40

As it is evident from the table above, both the configuration II and IV have a smaller percentage difference in the obtained value between String sum and array level IV. This represents a lower mismatch in the overall system. If the system were to perform under thermal mismatch and non uniformity, then the modules under high temperatures as compared to the modules experiencing cooler temperatures would have a lower power output. Typically high temperature modules (lower power) dictate the system power which would then lead to a large % difference. If there is uniformity in temperatures, then no matter if we measure individual strings or the entire array at one time, we should expect to achieve similar power output.

4.3.6 IR Imaging

For the last phase of the thesis, several IR images were taken for each configuration using a Fluke IR camera. The goal of IR imaging is to clearly identify thermal behavior in the system and to identify any potential hot spots developing in the system. In order to achieve sufficient thermal contrast in the

system, both arrays were individually shorted and left to achieve thermal equilibrium before an image was attempted. The images were attempted from a distance in order to capture the entire array and the camera was directed at an angle of approximately 15-20 º at the array[15]. An emissivity factor of 0.92 was chosen to replicate glass and minimize reflections from module surface.

The IR images are presented in the sections below:

4.3.6.1 IR Configuration I

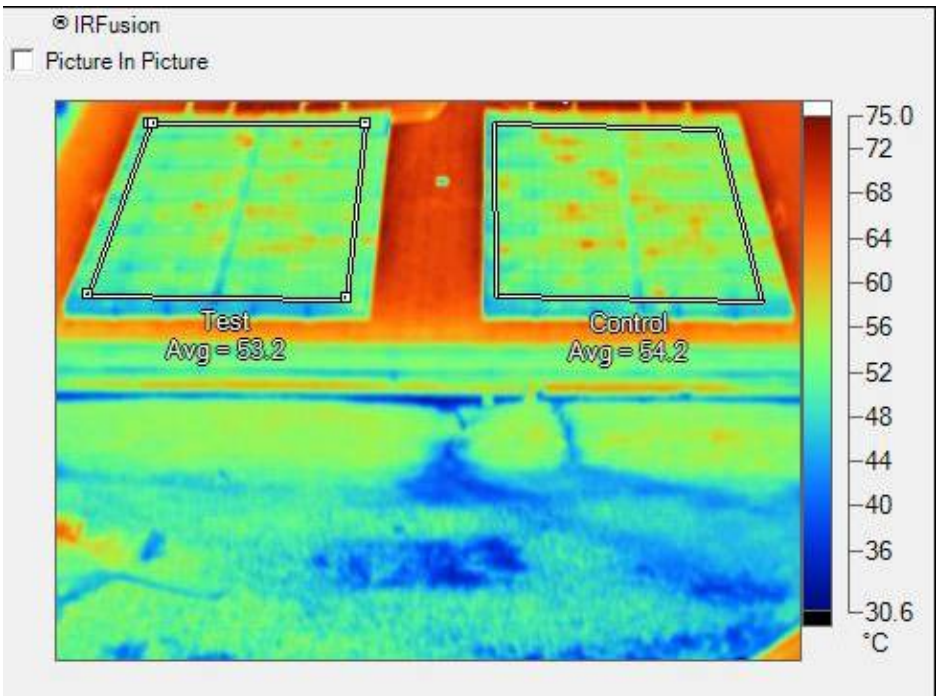

Image Info | Marker Data | Graph | Visible

Label	Emissivity	Background Temp	Min	Avg	Max	St. Dev.	Units
Test	0.92	35.0	43.6	53.2	62.8	2.35	°C
Control	0.92	35.0	44.1	54.2	64.2	2.53	°C

Figure 4.29 IR and Temperature Details (Configuration I)

4.3.6.2 IR Configuration II

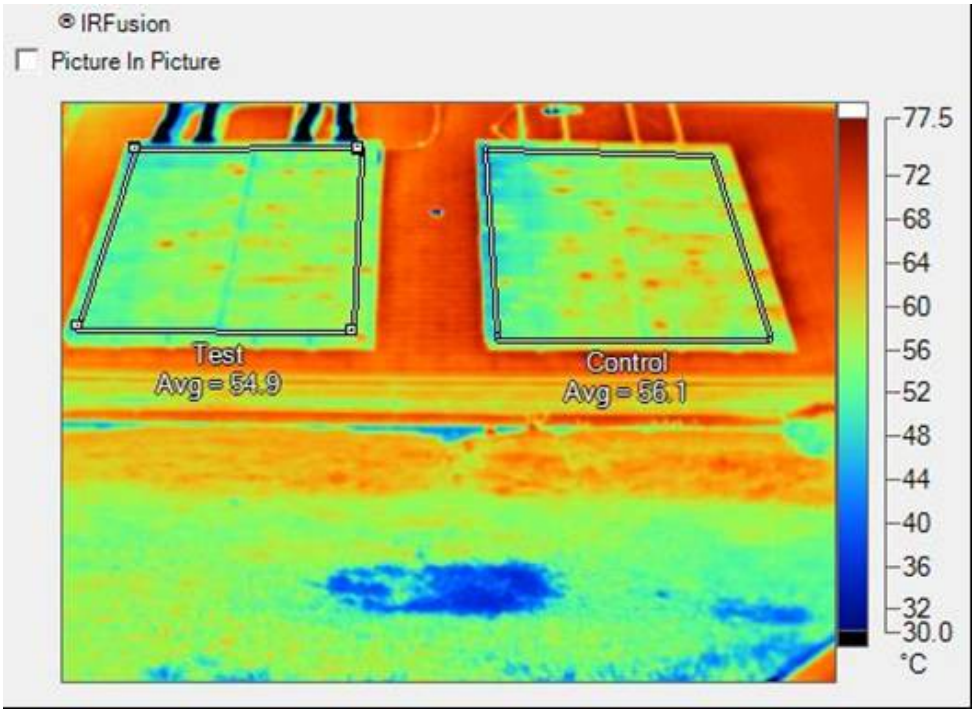

Image Info | Marker Data | Graph | Visible

Label	Emissivity	Background Temp	Min	Avg	Max	St. Dev.	Units
Test	0.92	36.6	45.6	54.9	66.6	2.27	°C
Control	0.92	36.6	44.1	56.1	67.3	2.94	°C

Figure 4.30 IR and Temperature Details (Configuration II)

4.3.6.3 IR configuration III

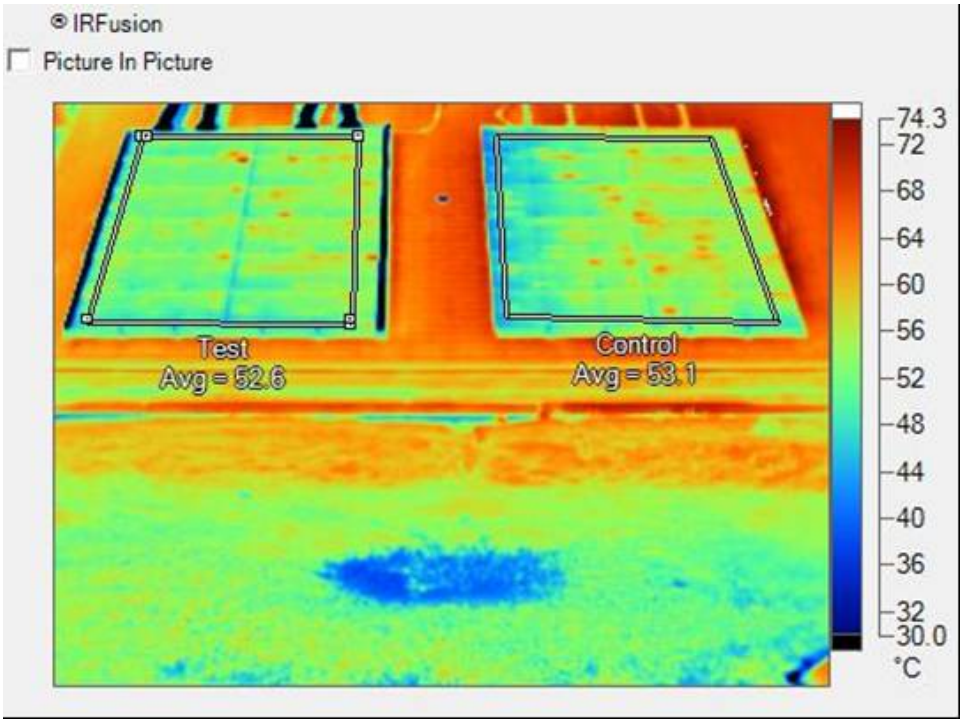

Image Info | Marker Data | Graph | Visible

Label	Emissivity	Background Temp	Min	Avg	Max	St. Dev.	Units
Test	0.92	34.8	44.5	52.6	68.3	2.29	°C
Control	0.92	34.8	42.8	53.1	63.6	2.94	°C

Figure 4.31 IR and Temperature Details (Configuration III)

4.3.6.4 IR configuration IV

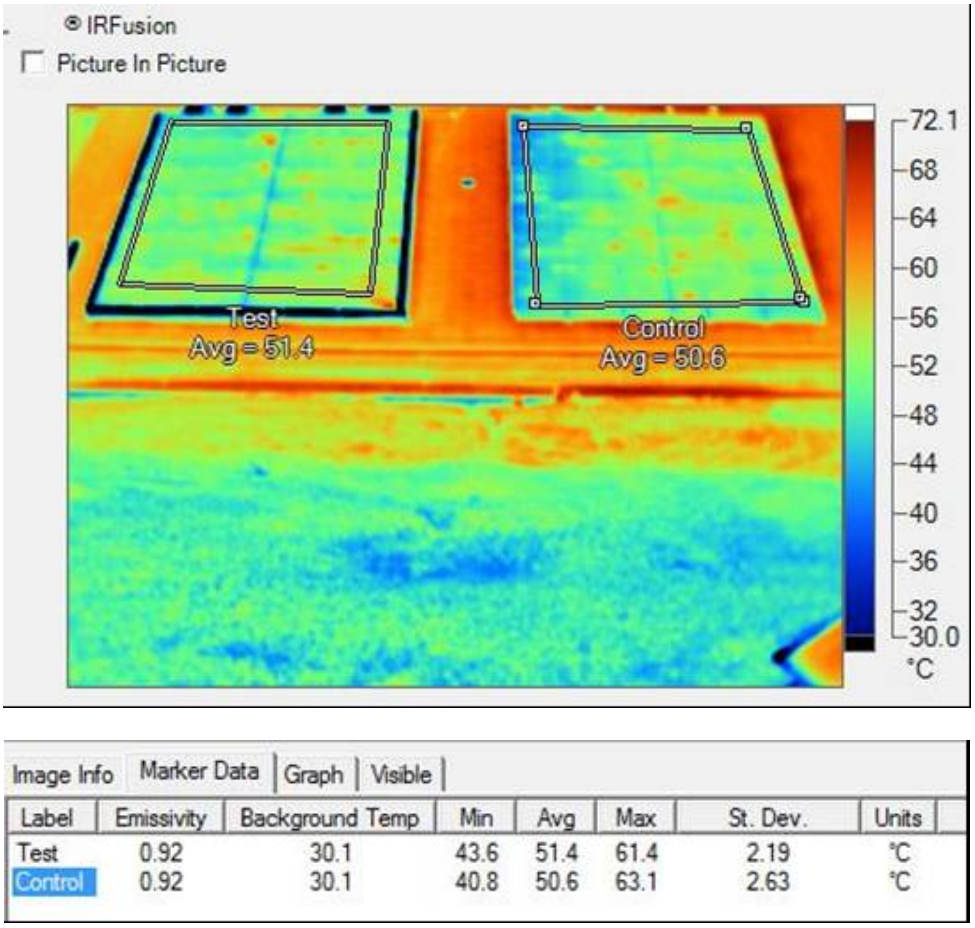

Image Info | Marker Data | Graph | Visible

Label	Emissivity	Background Temp	Min	Avg	Max	St. Dev.	Units
Test	0.92	30.1	43.6	51.4	61.4	2.19	°C
Control	0.92	30.1	40.8	50.6	63.1	2.63	°C

Figure 4.32 IR and Temperature Details (Configuration IV)

IR images help portray if there are any significant hot spot issues developing in the modules or hot patches that we must be concerned with. We are also able to analyze the cooler spots of the system by looking at the usual blue spots of the system as compared to the red zones. It is interesting to see from the configuration IV image (last setup) that the wind blocks are preventing any wind flow from sides and bottom, as a result the overall thermal distribution looks more uniform as compared to the control array where the left (facing North) portion of the array is experiencing cooler temperatures while the other half of the array is warmer. Also the wind blocks have caused the overall average temperature of

the test array to be about 1 ºC higher compared to control array. On a positive note, the temperature gap (max – min) for the test array is slightly lower (17.8 ºC) while it is (22.3ºC) for control.

CHAPTER 5

CONCLUSION & RECOMMENDATION

5.1 Conclusion

For this study, two side by side arrays under four different configurations have been conceptualized and the results are presented. The high operating temperatures certainly have a negative effect on the array as a whole, however all the modules do not experience identical temperatures at one particular point under identical ambient conditions. The temperature variability or simply known as the mismatch factor worsened under high wind conditions. An array experiencing high volatility in temperature mismatch would produce mixture of voltage in the modules which would lead to a mismatch in power (Pmax) from the individual modules. Typically the worst performing module would then be the lead in determining the array power. The effect of cooling the array with the fan has been evaluated along with several wind blocks. Although the fan did not prove to have any significant cooling effect on the system, but when combined with wind (wooden) blocks it helped improve the thermal mismatch both under low and high wind speed conditions(Lower standard deviation). Although the overall temperature of the test array in configuration IV increased slightly, the improvement in thermal mismatch compensated for the slight loss in power. Similarly, thermal model proved to be more accurate and less turbulent (lower deviation in coefficients) with configuration IV.

5.2 Recommendation

At present with the current setup of Configuration IV, thermal stability and better system temperature uniformity has been achieved. Moving forward it would be

best for the future student to experiment with different capacity fans to see if the stagnant thermal air mass can be affected in a more efficient manner. Different technique for air exhaust should be considered such as instead of pulling the hot air from top, it could be pushed from the bottom to see if it has any effect. Different approaches to air pulling underneath the system such as multiple ducts should be considered at different location points underneath the array for maximum air exhaust. Arrhenius reliability physical model can be introduced as an additional analysis on lifetime prediction for the array under test with fan operation. Lifetime prediction with fan cooling would be a value add moving forward.

REFERENCES

[1] Oh, Jaewon. *Building Applied and Back Insulated Photovoltaic Modules: Thermal Models.* Master's Thesis Report, Arizona State University (2010).

[2] Schams, Ben. *Effect of Air Gap on Building Applied Photovoltaic Modules: An Energy and Economic Analysis.* Master's Applied Project Report, Arizona State University (2010).

[3] Hrica, Jonathan. *Building Applied Photovoltaic Array: Thermal Modeling and Fan Cooling .* Master's Thesis Report, Arizona State University (2010).

[4] Honsberg, Christiana, and Bowden, Stuart. *PV CDROM – Modules And Arrays: PV Module Temperature (*2010), retrieved on August, 2011. http://pveducation.org/pvcdrom/modules/pv-module-temperature

[5] Honsberg, Christiana, and Bowden, Stuart. *PV CDROM – Modules And Arrays: Heat Generation in PV Modules (*2010), retrieved on August, 2011. http://pveducation.org/pvcdrom/modules/heat-generation-in-PV-module

[6] Honsberg, Christiana, and Bowden, Stuart. *PV CDROM – Modules And Arrays:Heat Loss in PV Modules (*2010), retrieved on August, 2011. http://pveducation.org/pvcdrom/modules/heat-loss-in-PV-modules

[7] King, D.L.,Boyson, W.E and Kratochvil, J.A. *PHOTOVOLTAIC ARRAY PERFORMANCE MODEL.* Albuquerque, New Mexico, Sandia National Laboratories, (2004).

[8] Messenger, Roger A., Ventre, Jerry. "*Photovoltaic Systems Engineering: Third Edition.*" (2010).

[9] Tang, Yingtang. *Outdoor Energy Rating of Photovoltaic Modules.* Master's Thesis Report, Arizona State University (2010).

[10] Lad, Radhika. *Outdoor Energy Rating of Photovoltaic Modules.* Master's Thesis Report, Arizona State University (2010).

[11] Shrestha, Bijay. *Temperature of Rooftop PV Modules: Effect of Air Gap and Ambient Condition* . Master's Thesis Report, Arizona State University (2009).

[12] Tripanagnostopoulos, Y, Souliotis,M , Battisti,R and Corrado, A. *Application Aspect of Hybrid PVT/Air Solar Systems*. Physics Department, University of Patras, Patra 26500, Greece

[13] “*The More Complete Solar Energy System*”, echo solar system, http://echofirst.com/whatisecho.php (2011)

[14] Dunlop, James P. “*Photovoltaic Systems: Second Edition*”. (2010)

[15] “*Thermal imaging cameras: a fast and reliable tool for testing solar panels*” FLIR, www.flir.com, (2011), retrieved on September 2011

APPENDIX A

STC DATA PLOTS FOR ROW LEVEL I-V

(CONFIGURATION I, II & IV)

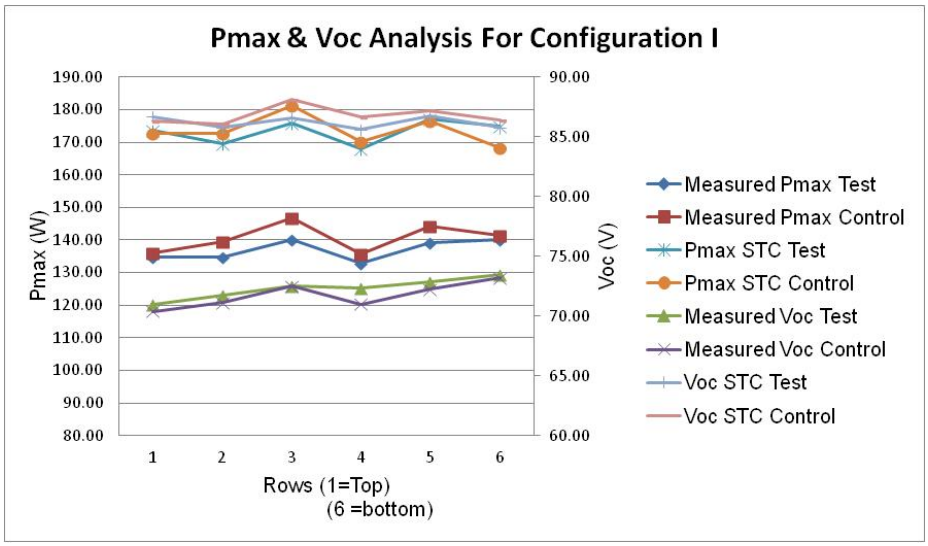
Pmax & Voc Analysis For Configuration I
Pmax (W)
Voc (V)
Rows (1=Top)
(6 =bottom)
Measured Pmax Test
Measured Pmax Control
Pmax STC Test
Pmax STC Control
Measured Voc Test
Measured Voc Control
Voc STC Test
Voc STC Control

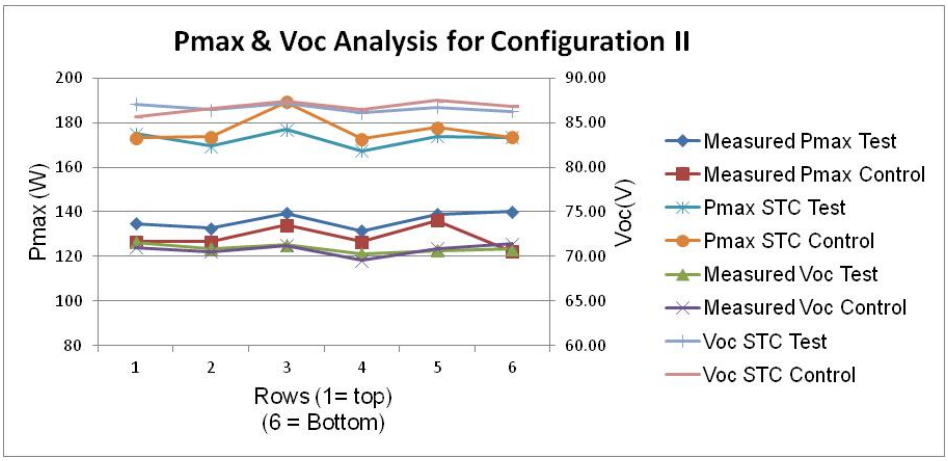
Pmax & Voc Analysis for Configuration II
Pmax (W)
Voc(V)
Rows (1= top)
(6 = Bottom)
Measured Pmax Test
Measured Pmax Control
Pmax STC Test
Pmax STC Control
Measured Voc Test
Measured Voc Control
Voc STC Test
Voc STC Control

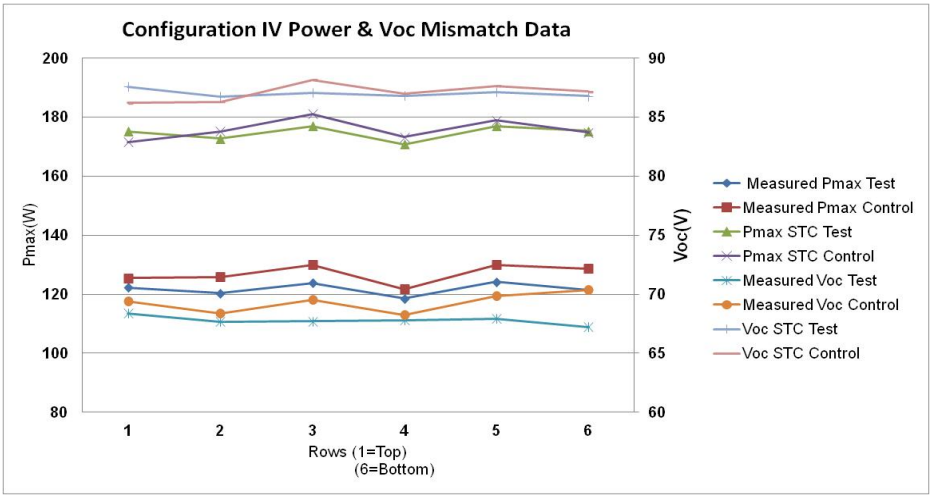
Configuration IV Power & Voc Mismatch Data
Pmax(W)
Voc(V)
Rows (1=Top)
(6=Bottom)
Measured Pmax Test
Measured Pmax Control
Pmax STC Test
Pmax STC Control
Measured Voc Test
Measured Voc Control
Voc STC Test
Voc STC Control